# Supporting Information

# α-Pyrones from the Marine-Derived Actinomycete *Nocardiopsis dassonvillei* subsp. *dassonvillei* XG-8-1

Peng Fu, Peipei Liu, Qianhong Gong, Yi Wang, Pei Wang, and Weiming Zhu*

*Key Laboratory of Marine Drugs, Ministry of Education of China, School of Medicine and Pharmacy, Ocean University of China, Qingdao 266003, Peoples' Republic of China*

## List of Supporting Information

**The 16S rRNA gene sequences data of *Nocardiopsis dassonvillei* subsp. *dassonvillei* XG-8-1**

ACACATGCAGTCGAGCGGTAAGGCCCTTCGGGGTACACGAGCGGCGAACGGGTGAGTA
ACACGTGAGCAACCTGCCCCTGACTCTGGGATAAGCGGTGGAAACGCCGTCTAATACC
GGATACGACCCGCCACCTCATGGTGGAGGGTGGAAAGTTTTTCGGTCAGGGATGGGCTC
GCGGCCTATCAGCTTGTTGGTGGGGTAACGGCCTACCAAGGCGATTACGGGTAGCCGGC
CTGAGAGGGCGACCGGCCACACTGGGACTGAGACACGGCCCAGACTCCTGCGGGAGGC
AGCAGTGGGGAATATTGCGCAATGGGCGAAAGCCTGACGCAGCGACGCCGCGTGGGGG
ATGACGGCCTTCGGGTTGTAAACCTCTTTTACCACCAACGCAGGCTTCCAGTTCTCTGGA
GGTTGACGGTAGGTGGGGAATAAGGACCGGCTAACTACGTGCCAGCAGCCGCGGTAAT
ACGTAGGGTCCGAGCGTTGTCCGGAATTATTGGGCGTAAAGAGCTCGTAGGCGGCGTGT
CGCGTCTGCTGTGAAAGACCGGGGCTTAACTCCGGTTCTGCAGTGGATACGGGCATGCT
AGAGGTAGGTAGGGGAGACTGGAATTCCTGGTGTAGCGGTGAAATGCGCAGATATCAG
GAGGAACACCGGTGGCGAAGGCGGGTCTCTGGGCCTTACCTGACGCTGAGGAGCGAAA
GCATGGGGAGCGAACAGGATTAGATACCCTGGTAGTCCATGCCGTAAACGTTGGGCGC
TAGGTGTGGGGGACTTTCCACGGTTTCCGCGCCGTAGCTAACGCATTAAGCGCCCCGCC
TGGGGAGTACGGCCGCAAGGCTAAAACTCAAAGGAATTTGACGGGGGCCCGCACAAGC
GGCGGAGCATGTTGCTTATTCGACGCACGCGAAGAACCTTACCAAGGTTTGACATCACC
CGTGGACTCGCAGAGATGTGAGGTCATTTAGTTGGCGGGTGACAGGTGGTGCATGGCTG
TCGTCAGCTCGTGTCGTGAGATGTTGGGTTAAGTCCCGCAACGAGCGCAACCCTTGTTC
CATGTTGCCAGCACGTAATGGTGGGGACTCATGGGAGACTGCCGGGGTCAACTCGGAG
GAAGGTGGGGATGACGTCAAGTCATCATGCCCCTTATGTCTTGGGCTGCAAACATGCTA
CAATGGCCGGTACAATGGGCGTGCGATACCGTAAGGTGGAGCGAATCCCTAAAAGCCG
GTCTCAGTTCGGATTGGGGTCTGCAACTCGACCCCATGAAGGTGGAGTCGCTAGTAATC
GCGGATCAGCAACGCCGCGGTGAATACGTTCCCGGGCCTTGTACACACCGCCCGTCACG
TCATGAAAGTCGGCAACACCCGAAACTTGCGGCCTAACCCCTTGTGGGAGGGAGTGAG
TGAAGGTGGGGCTGGCGATTGGGACGAAGTCGTAACAAGGTAGCCGTACCGGAAGGTG
CGGCTGGATCACCTCCT

## The phylogenetic tree of *Nocardiopsis dassonvillei* subsp. *dassonvillei* XG-8-1

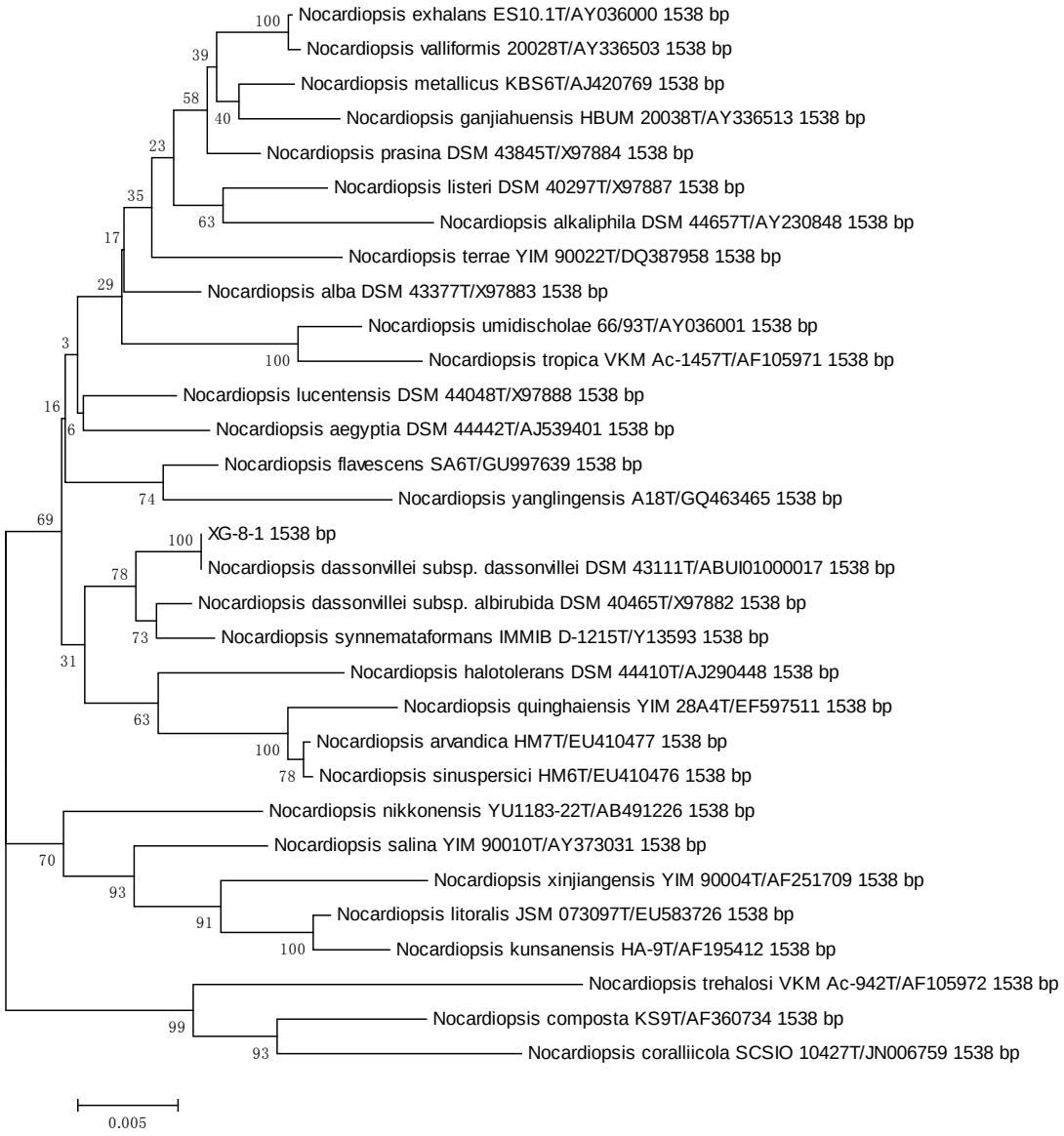


## Bioassay Protocols

**Cytotoxic Assays**. Cytotoxicity was assayed by the MTT[22] and SRB methods.[23] In the MTT assay, HL-60 cell line was grown in RPMI-1640 supplemented with 10% FBS under a humidified atmosphere of 5% $CO_2$ and 95% air at 37 °C. Cell suspension, 200 $\mu$L, at a density of $5 \times 10^4$ cell $mL^{-1}$ was plated in 96-well microtiter plates and incubated for 24 h. Then, 2 $\mu$L of the test solutions (in MeOH) were added to each well and further incubated for 72 h. The MTT solution (20 $\mu$L, 5 mg/mL in IPMI-1640 medium) was then added to each well and incubated for 4 h. Old medium containing MTT (150 $\mu$L) was then gently replaced by DMSO and pipetted to dissolve any formazan

crystals formed. Absorbance was then determined on a Spectra Max Plus plate reader at 540 nm. In the SRB assay, 200 $\mu$L of the A549 cell suspension was plated in 96-well plates at a density of 2 × $10^5$ cell $mL^{-1}$. Then, 2 $\mu$L of the test solutions (in MeOH) were added to each well and the culture was further incubated for 24 h. The cells were fixed with 12% trichloroacetic acid and the cell layer stained with 0.4% SRB. The absorbance of the SRB solution was measured at 515 nm. VP-16 (etoposide) was used as the positive control with the $IC_{50}$ values of 0.042 and 0.63 $\mu$M, respectively.

**Antimicrobial Assays**. The antimicrobial activities against *Escherichia coli*, *Bacillus subtilis*, *Pseudomonas aeruginosa*, *Enterobacter aerogenes*, *Staphylococcus aureus*, and *Candida albicans* were evaluated by an agar dilution method.[24] The tested strains were cultivated in LB agar plates for bacteria and in YPD agar plates for *Candida albicans* at 37 °C. Compounds **1**–**7** and positive controls were dissolved in MeOH at different concentrations by the continuous 2-fold dilution methods. A 10 $\mu$L quantity of test solution was absorbed by a paper disk (5 mm diameter) and placed on the assay plates. After 24 h incubation, zones of inhibition (mm in diameter) were recorded. The minimum inhibitory concentrations (MICs) were defined as the lowest concentration at which no microbial growth could be observed. Ciprofloxacin lactate and ketoconazole was used as positive control for *Escherichia coli*, *Bacillus subtilis*, *Pseudomonas aeruginosa*, *Enterobacter aerogenes*, *Staphylococcus aureus*, and *Candida albicans* with MIC values of 0.24, 0.94, 0.47, 0.47, 3.78 and 0.15 $\mu$M, respectively.

**Anti-Quorum Sensing (QS) Activity Assays**. 15 mL of warm molten LB agar were seeded with 0.2 mL overnight culture of *P. aeruginosa* QSIS-*lasI*. Sucrose, Gentamicin (Sigma), 3-oxo-C12-HSL (Sigma), and 2,3,5-triphenyltetrazolium chloride (TTC, Sigma) were added to the final concentrations of 6%, 80 $\mu$g/mL, 20 nM, and 0.025% (wt/vol), respectively. Then the mixed culture solution was immediately poured into a Petri dish. Samples were pipetted into wells punched in the solidified agar with a sterile cork borer.[25] Plates were incubated overnight at 37 °C and examined for living bacteria around the well. The growth of QSIS-*lasI* is seen as a red zone of triphenyl formazan around the wells containing anti-QS compounds (positive control furanone C30).

Well diffusion assay of *Chromobacterium violaceum* CV026 was subjected in a similar way except that the mixed LB agar contained 0.2 mL overnight culture of *C. violaceum* CV026, 500 nM *N*-hexanoylhomoserine lactone (Cayman) and 50 $\mu$g/mL kanamycin (Sigma).[26] Plates were incubated overnight at 30 °C and examined for white zone around the wells containing anti-QS compounds.

## Theory and Calculation Details

The calculations were performed by using the density functional theory (DFT) as carried out in the Gaussian 03.[20] The preliminary conformational distributions search was performed by HyperChem 7.5 software. All ground-state geometries were optimized at the B3LYP/6-31G(d) level. Solvent effects of methanol solution were evaluated at the same DFT level by using the SCRF/PCM method.[S1] TDDFT[S2] at B3LYP/6-31G(d) was employed to calculate the electronic excitation energies and rotational strengths in methanol.

(S1) (a) Miertus, S.; Tomasi, J. *Chem. Phys.* **1982**, *65*, 239–245. (b) Tomasi, J.; Persico, M. *Chem. Rev.* **1994**, *94*, 2027–2094. (c) Cammi, R.; Tomasi, J. *J. Comp. Chem.* **1995**, *16*, 1449–1458.

(S2) (a) Casida, M. E. In Recent Advances in Density Functional Methods, part I; Chong, D. P., Eds.; World Scientific: Singapore, 1995; pp 155–192. (b) Gross, E. K. U.; Dobson, J. F.; Petersilka, M. Top. *Curr. Chem.* **1996**, *181*, 81–172. (c) Gross, E. K. U.; Kohn, W. Adv. Quantum Chem. **1990**, *21*, 255–291. (d) Runge, E.; Gross, E. K. U. *Phys. Rev. Lett.* **1984**, *52*, 997–1000.

**Table S1. The atom coordinates of the lowest energy conformer of compound 2**

| | | | | | | | |
|---|---|---|---|---|---|---|---|
| C | 1.7426 | 0.35153 | -0.31758 | H | 3.05539 | -1.72733 | 0.47972 |
| C | 1.05429 | 1.45563 | -0.73193 | H | 5.55036 | -1.96059 | 0.12424 |
| C | -0.34552 | 1.35109 | -0.98185 | H | 5.21442 | -1.52254 | 1.79174 |
| C | -1.03018 | 0.18165 | -0.81415 | H | 5.81265 | -0.29359 | 0.66441 |
| C | -0.29015 | -1.0039 | -0.39968 | H | 3.88313 | 1.94684 | -1.21994 |
| O | 1.08009 | -0.82543 | -0.15996 | H | 3.55542 | 2.37134 | 0.46244 |
| O | -0.73281 | -2.12193 | -0.24667 | H | 5.00701 | 1.45708 | 0.04912 |
| C | 3.18026 | 0.29136 | -0.01293 | H | -2.87632 | 0.92749 | -1.57354 |
| C | 3.72437 | -0.87466 | 0.39623 | H | -2.60903 | -0.79822 | -1.82564 |
| C | 5.14998 | -1.1571 | 0.75758 | H | -3.00862 | -1.22465 | 0.59302 |
| C | 3.94952 | 1.58049 | -0.18791 | H | -3.63161 | 1.76458 | 0.65006 |
| C | -2.50148 | 0.01327 | -1.0931 | H | -4.46722 | 0.65497 | 1.71627 |
| C | -3.42178 | -0.33081 | 0.10975 | H | -2.58428 | 1.64639 | 2.93265 |
| C | -3.5285 | 0.79614 | 1.16316 | H | -2.28102 | -0.08421 | 2.71971 |
| C | -2.38673 | 0.86798 | 2.18577 | H | -1.42387 | 1.09443 | 1.71951 |
| C | -4.81701 | -0.68632 | -0.43044 | H | -5.48221 | -1.00533 | 0.38014 |
| H | 1.56434 | 2.39949 | -0.86948 | H | -4.76752 | -1.5002 | -1.16301 |
| H | -0.88279 | 2.23708 | -1.3141 | H | -5.28445 | 0.17779 | -0.9219 |

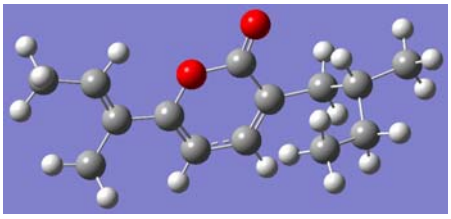

The lowest energy conformer of compound **2**

**Figure S1**. The $^{1}$H NMR spectrum of nocapyrone H (**1**) in $CDCl_3$ (600 MHz)

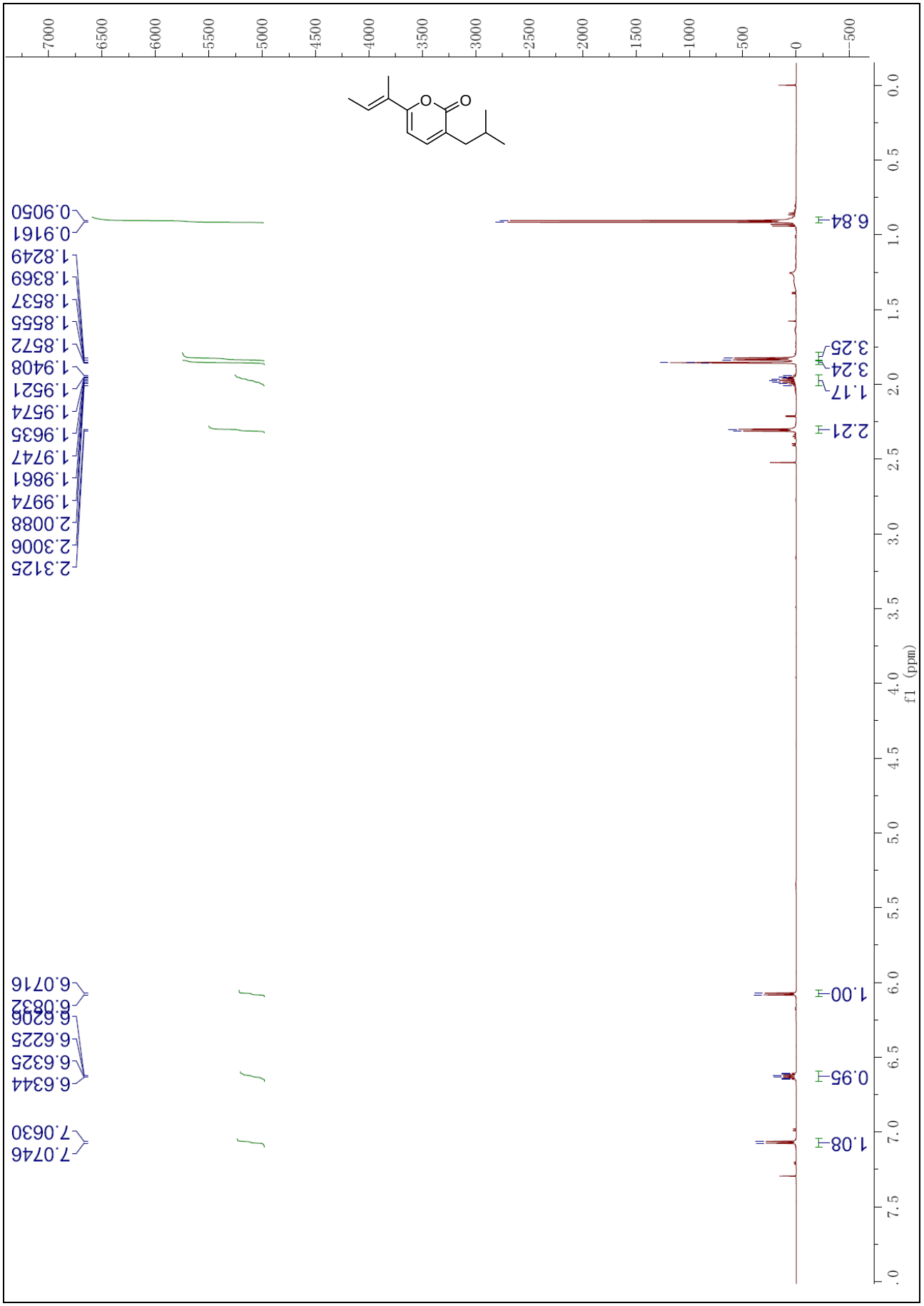

**Figure S2**. The $^{13}C$ NMR spectrum of nocapyrone H (**1**) in $CDCl_3$ (150 MHz)

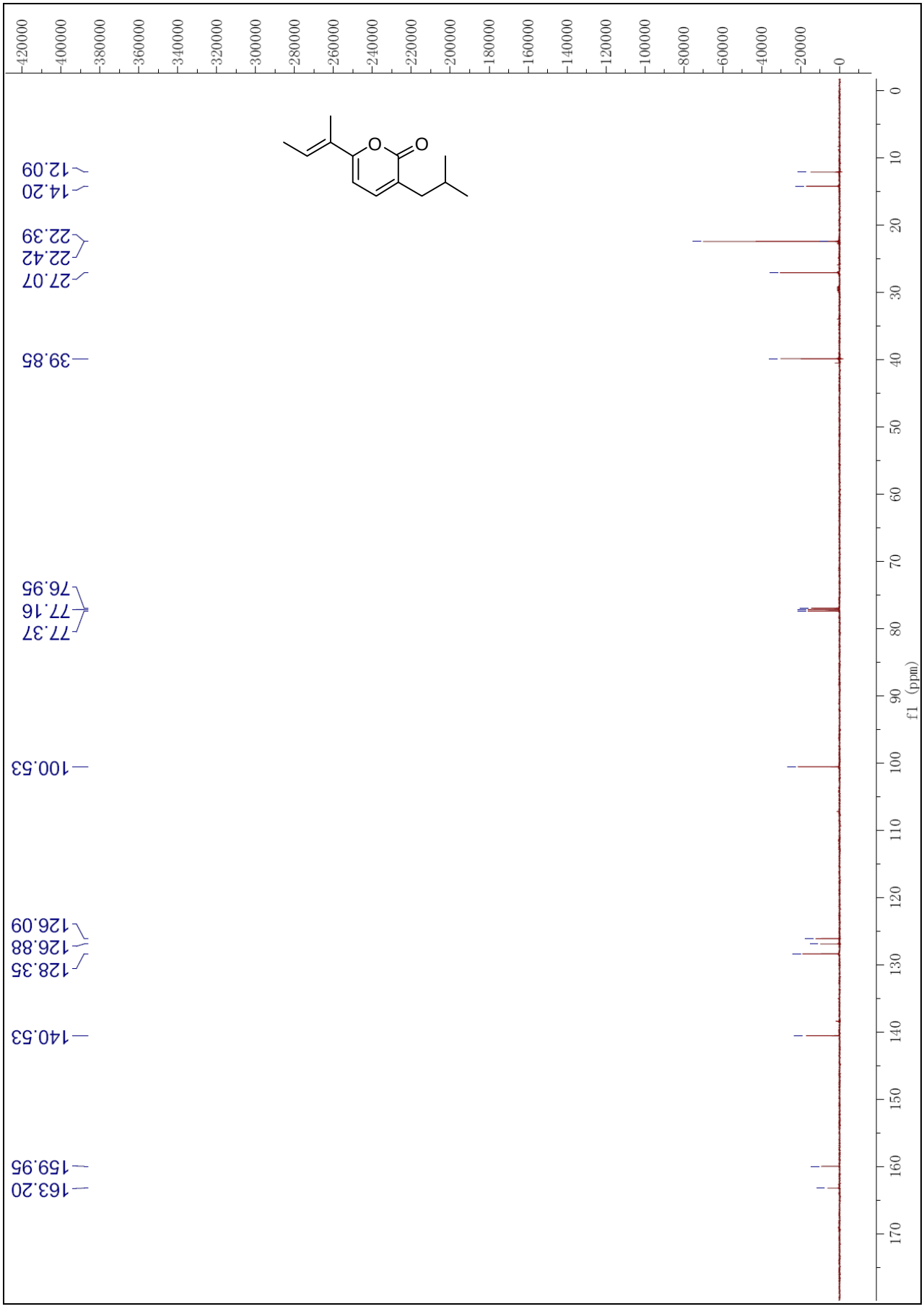

**Figure S3**. The DEPT spectrum of nocapyrone H (**1**) in $CDCl_3$ (150 MHz)

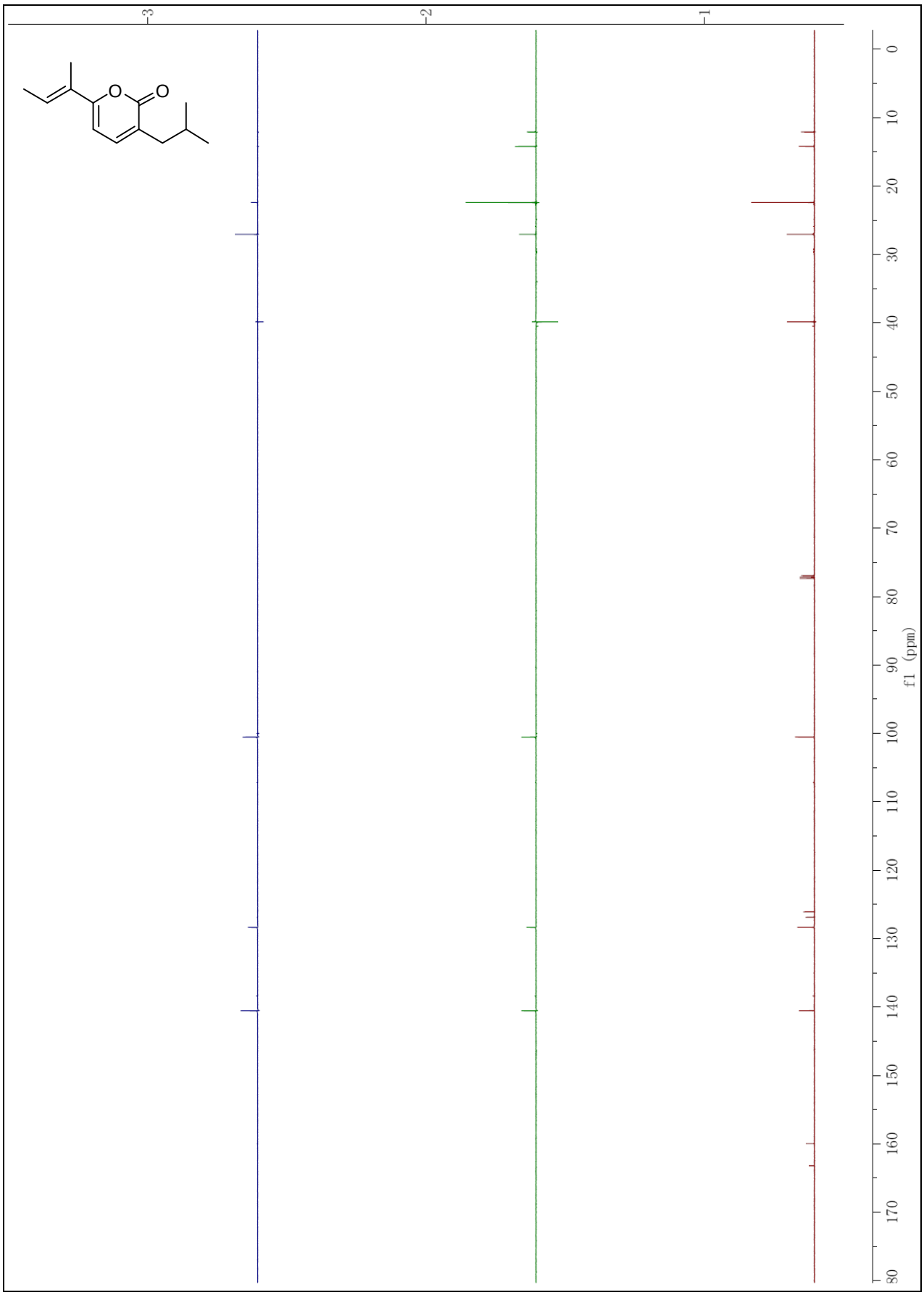

**Figure S4**. The HMQC spectrum of nocapyrone H (**1**) in $CDCl_3$ (600 × 150 MHz)

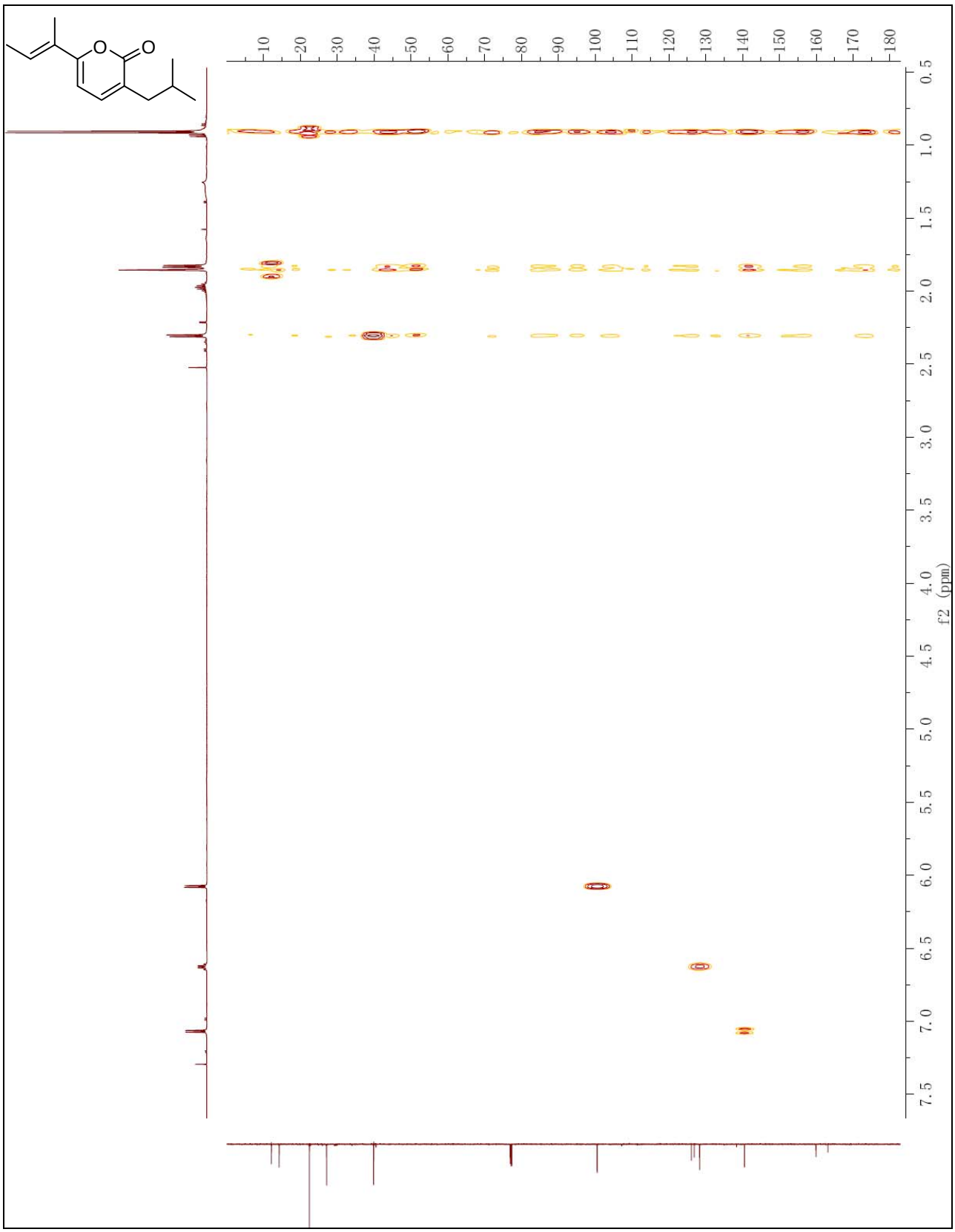

**Figure S5**. The $^{1}$H-$^{1}$H COSY spectrum of nocapyrone H (**1**) in $CDCl_3$ (600 MHz)

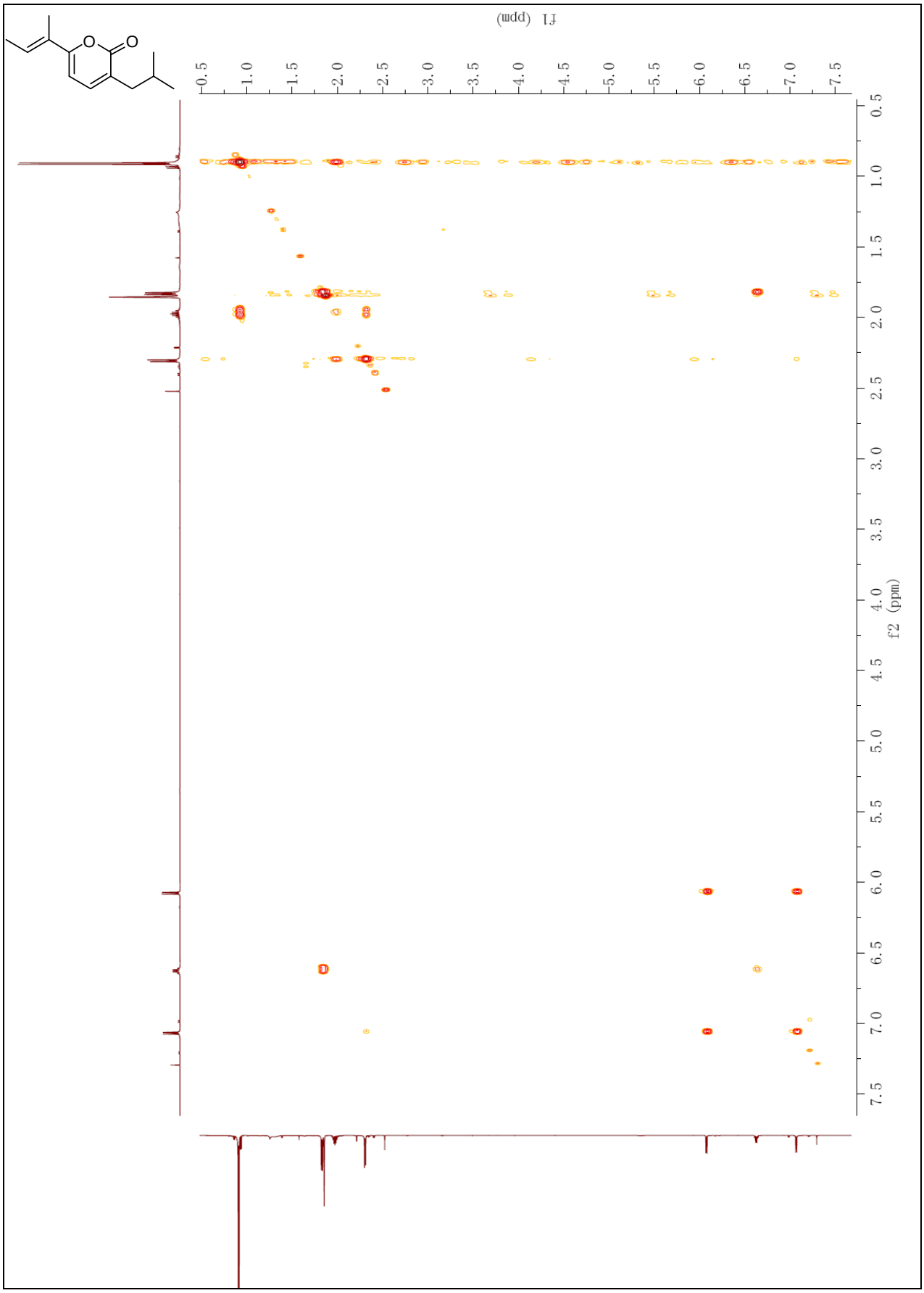

**Figure S6**. The HMBC spectrum of nocapyrone H (**1**) in $CDCl_3$ (600 × 150 MHz)

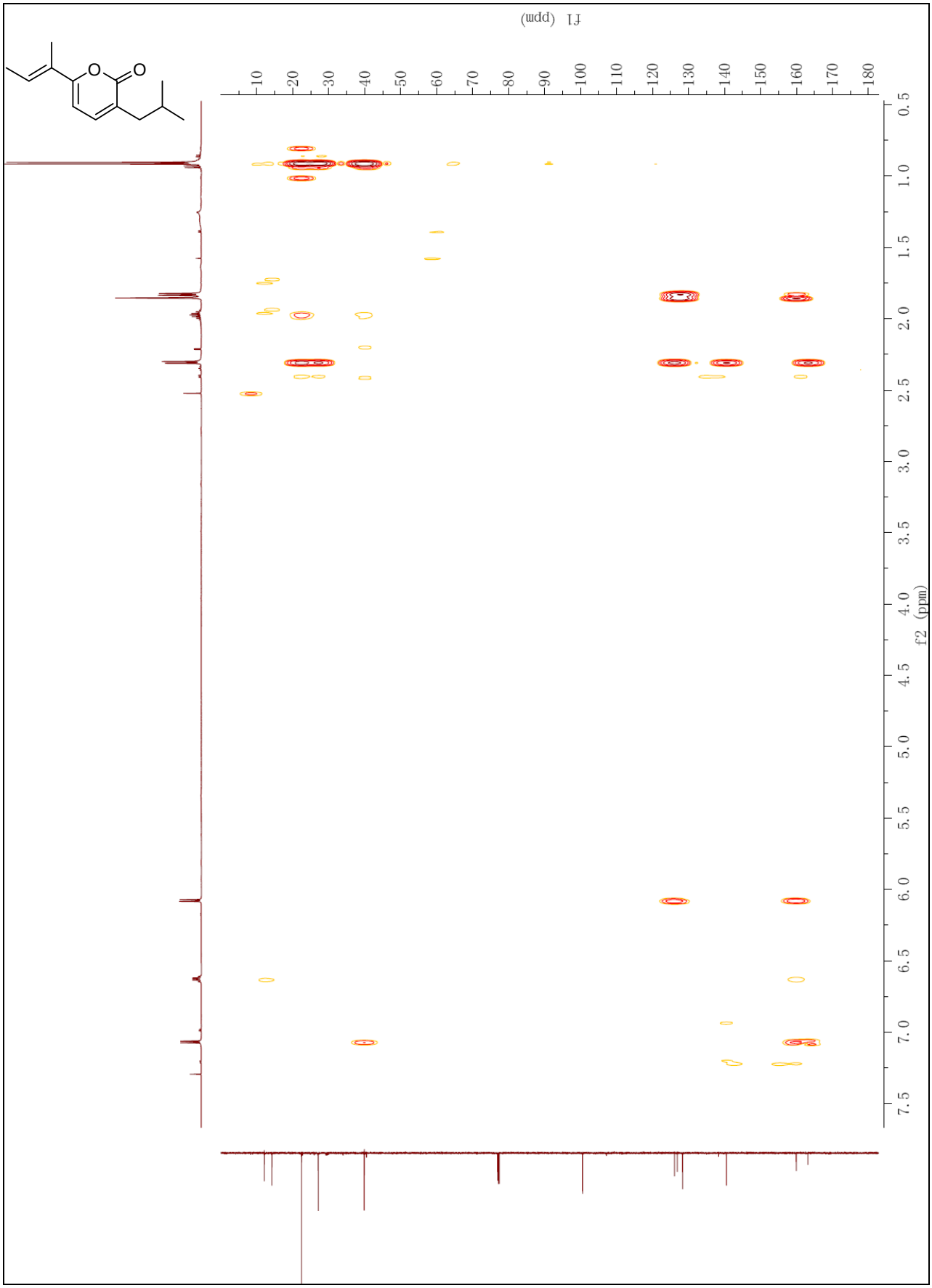

**Figure S7**. The NOE difference spectrum of nocapyrone H (**1**) in $CDCl_3$ (500 MHz)

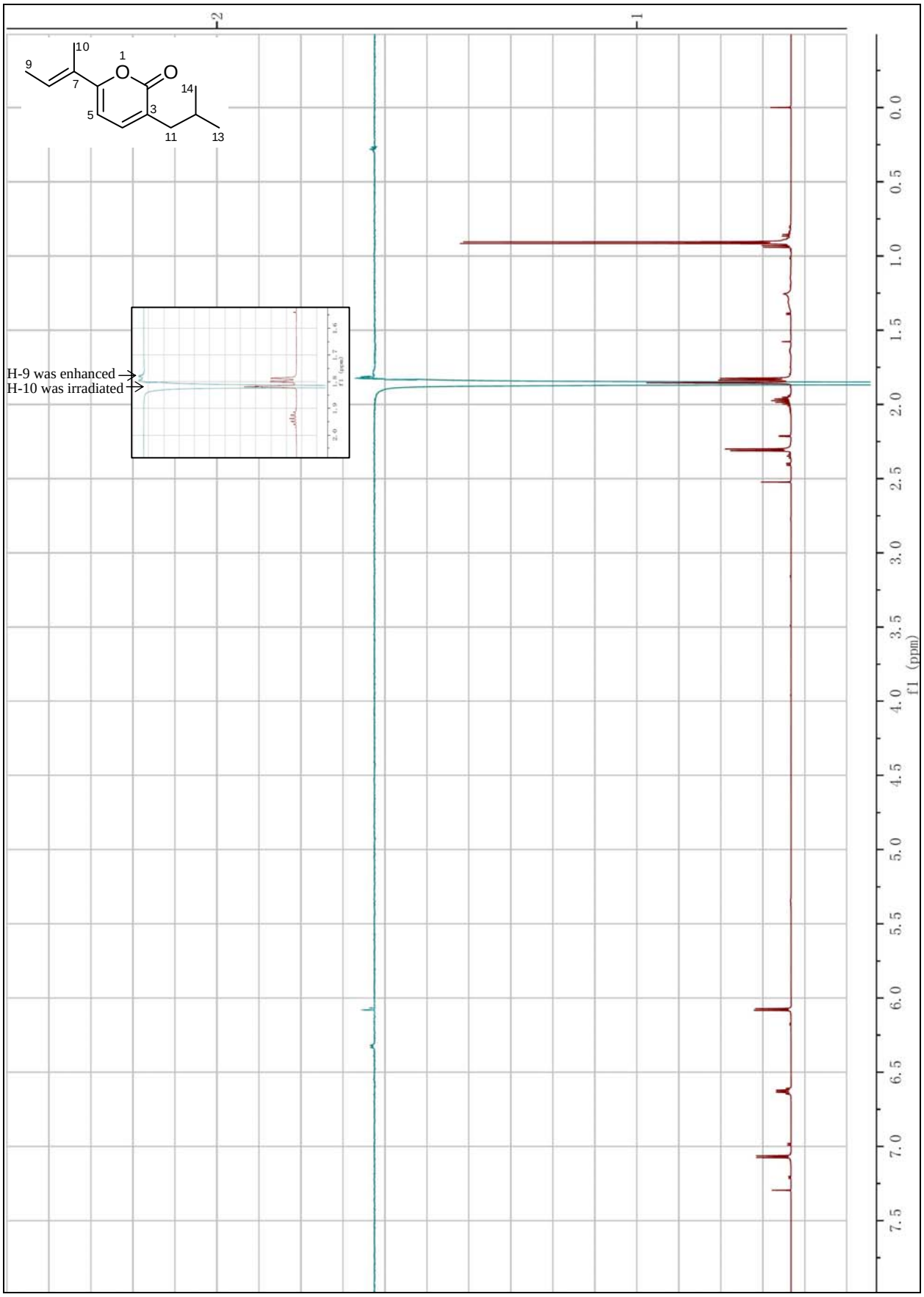

**Figure S8**. The $^{1}$H NMR spectrum of nocapyrone I (**2**) in $CDCl_3$ (600 MHz)

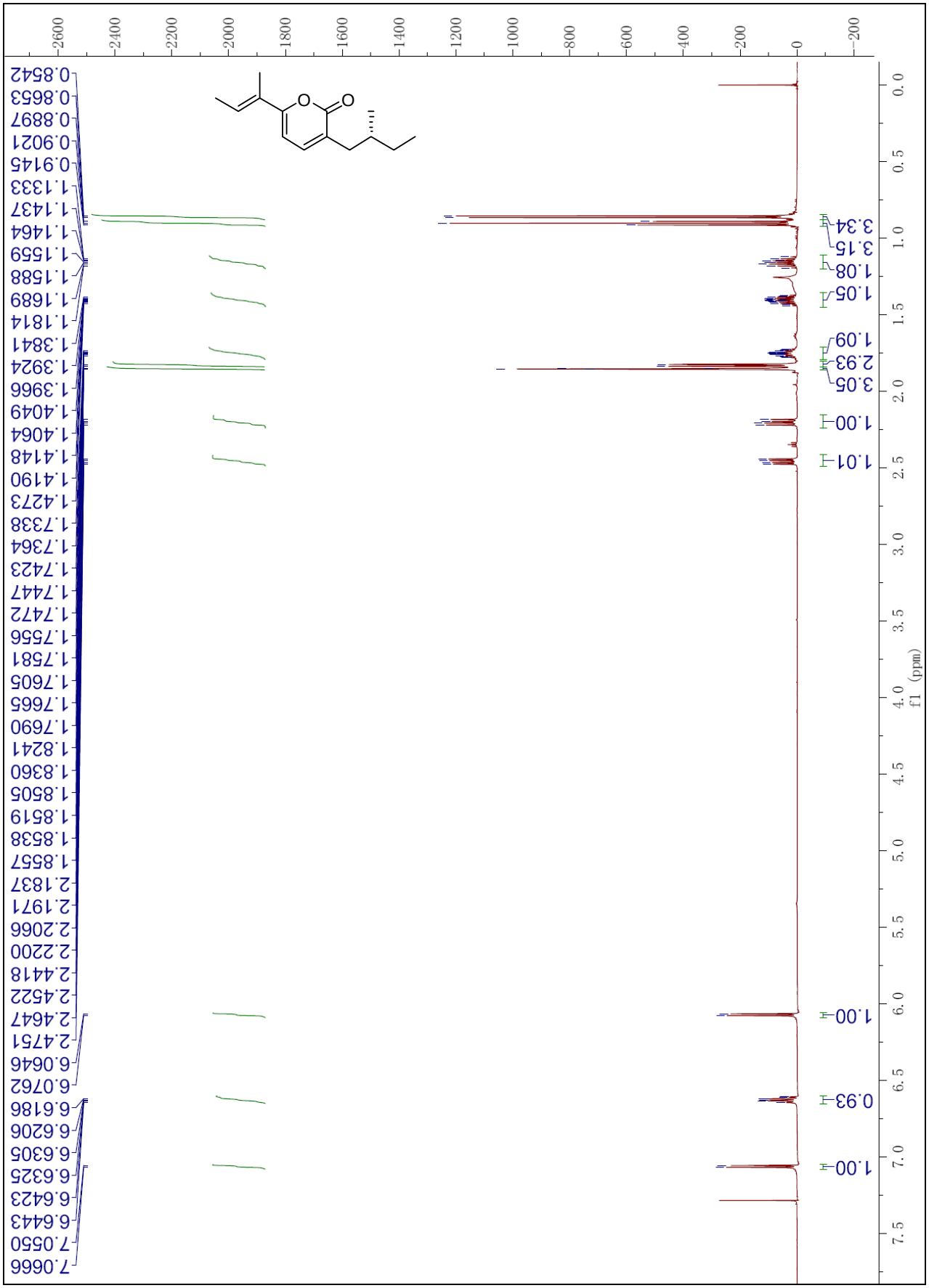

**Figure S9**. The $^{13}C$ NMR spectrum of nocapyrone I (**2**) in $CDCl_3$ (150 MHz)

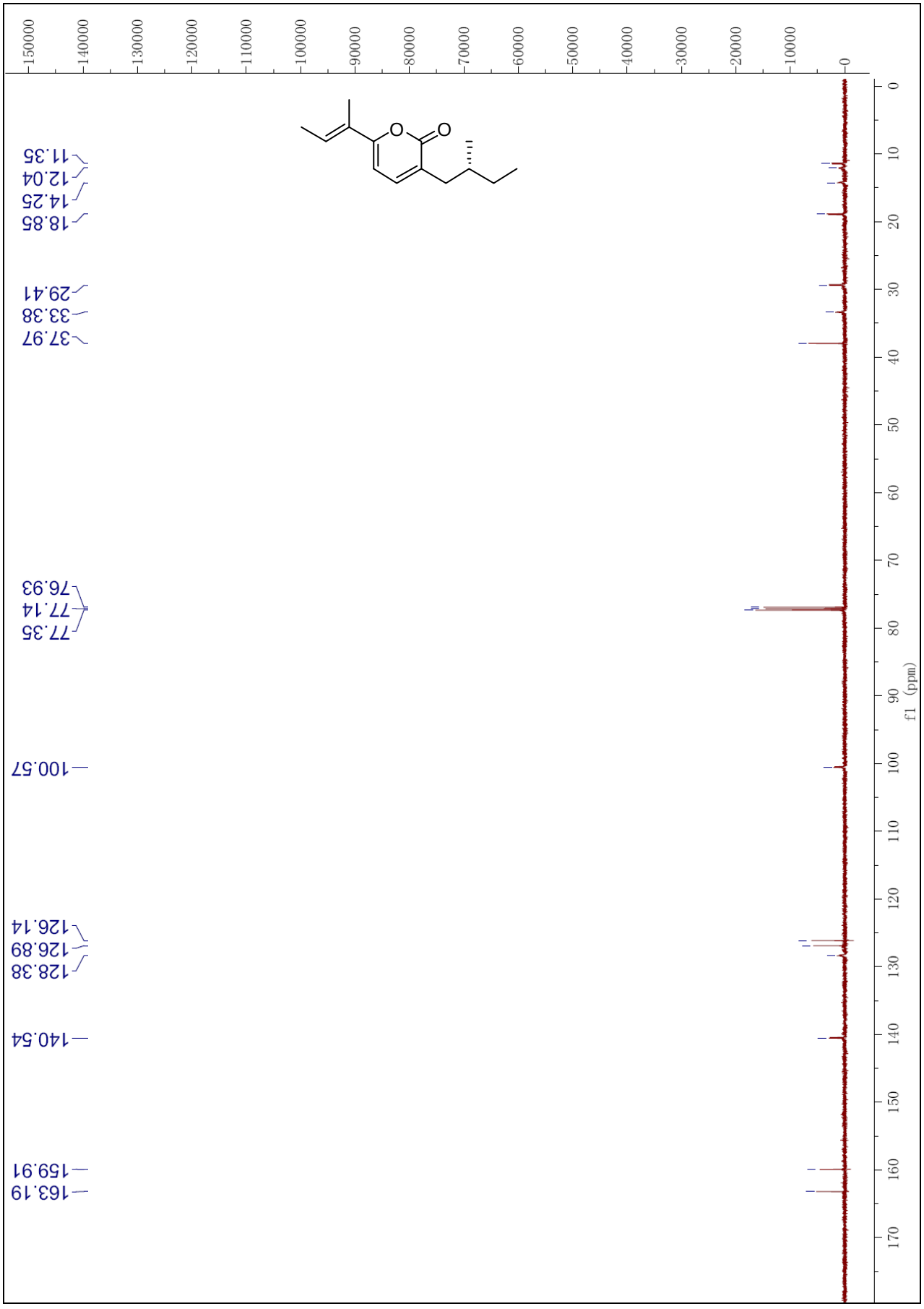

**Figure S10**. The DEPT spectrum of nocapyrone I (**2**) in $CDCl_3$ (150 MHz)

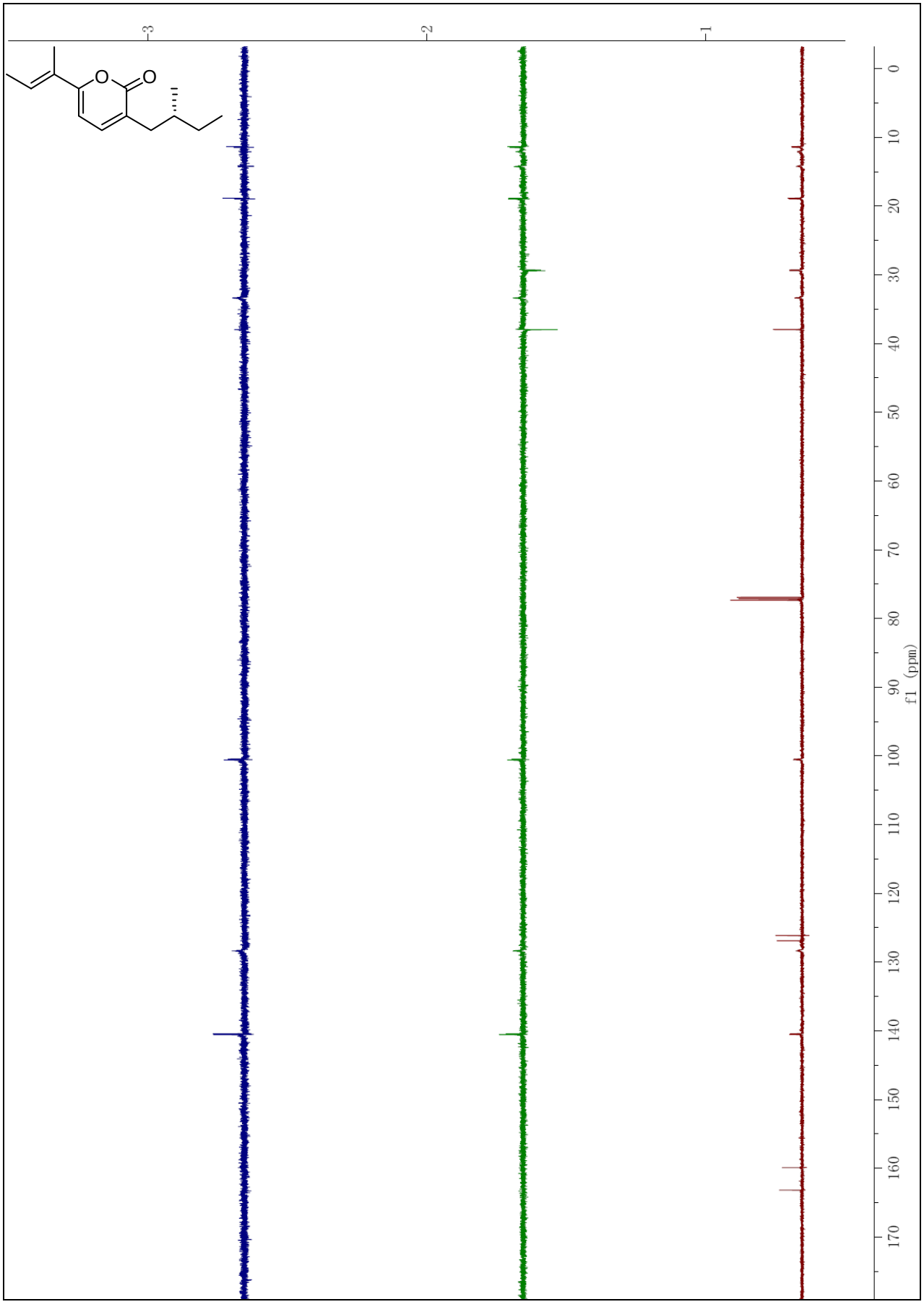

**Figure S11**. The $^{1}$H NMR spectrum of nocapyrone J (**3**) in $CDCl_3$ (600 MHz)

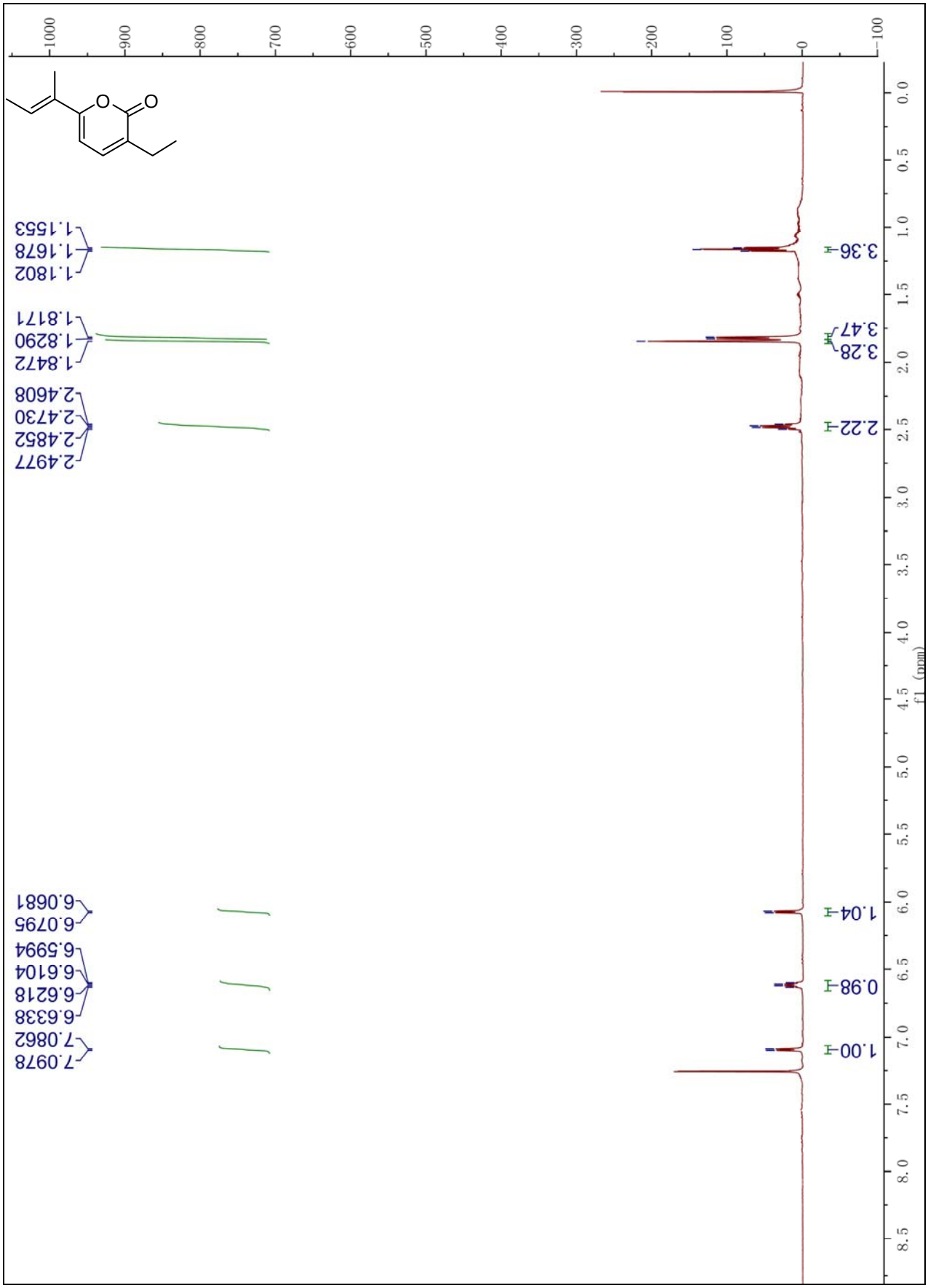

**Figure S12**. The $^{13}C$ NMR spectrum of nocapyrone J (**3**) in $CDCl_3$ (150 MHz)

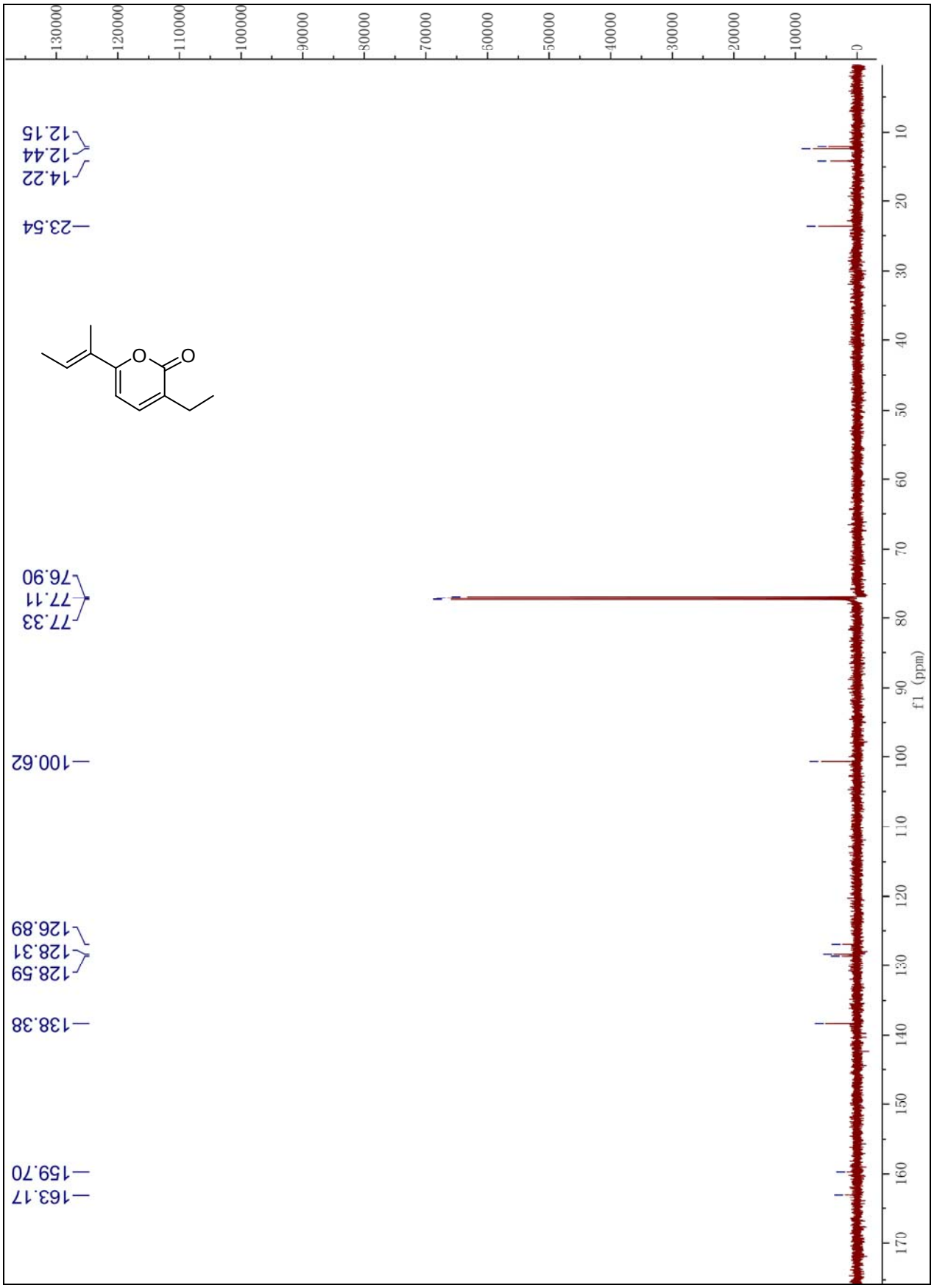

**Figure S13**. The DEPT spectrum of nocapyrone J (**3**) in $CDCl_3$ (150 MHz)

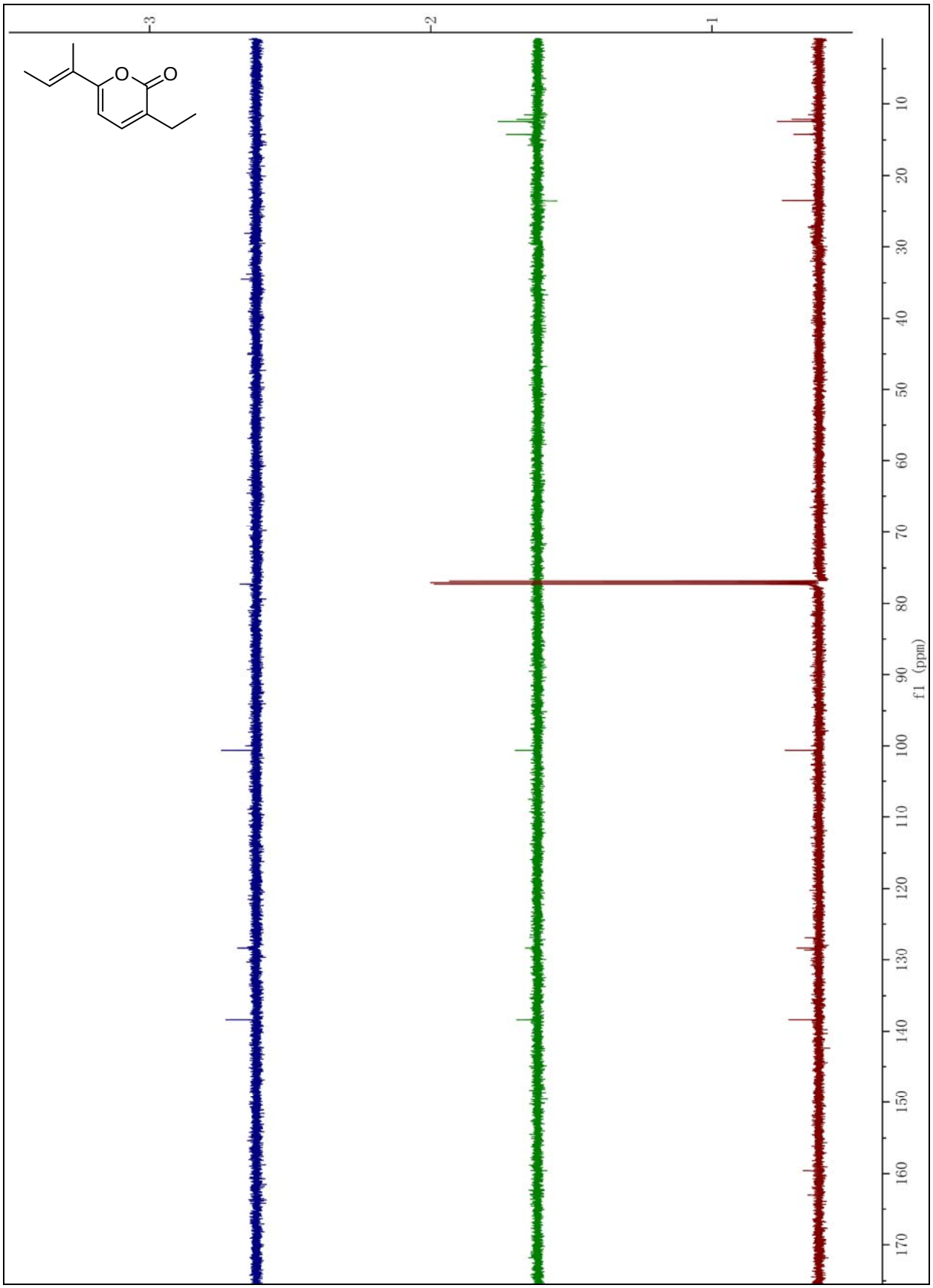

**Figure S14**. The $^{1}$H NMR spectrum of nocapyrone K (**4**) in $CDCl_3$ (600 MHz)

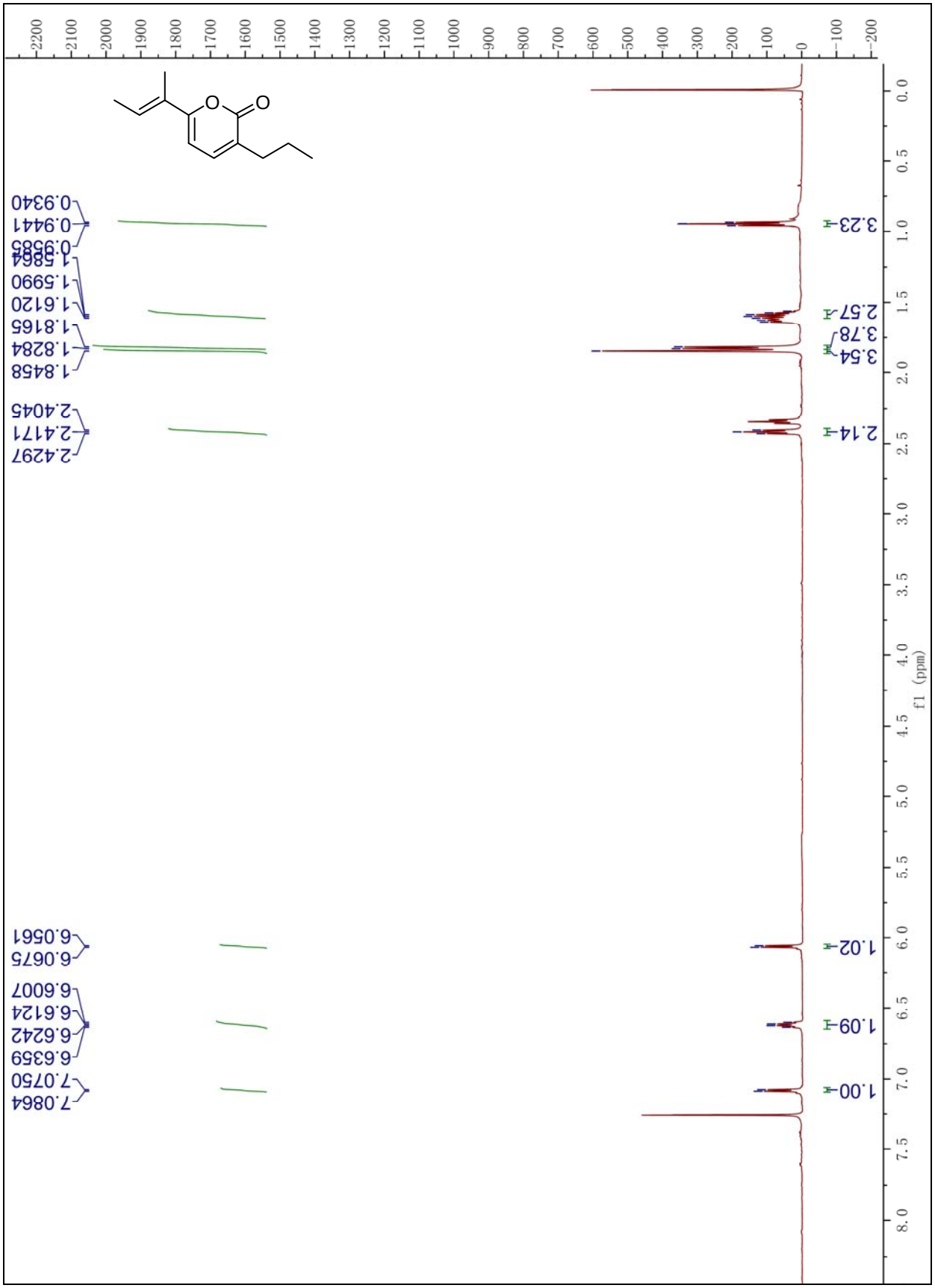

**Figure S15**. The $^{13}C$ NMR spectrum of nocapyrone K (**4**) in $CDCl_3$ (150 MHz)

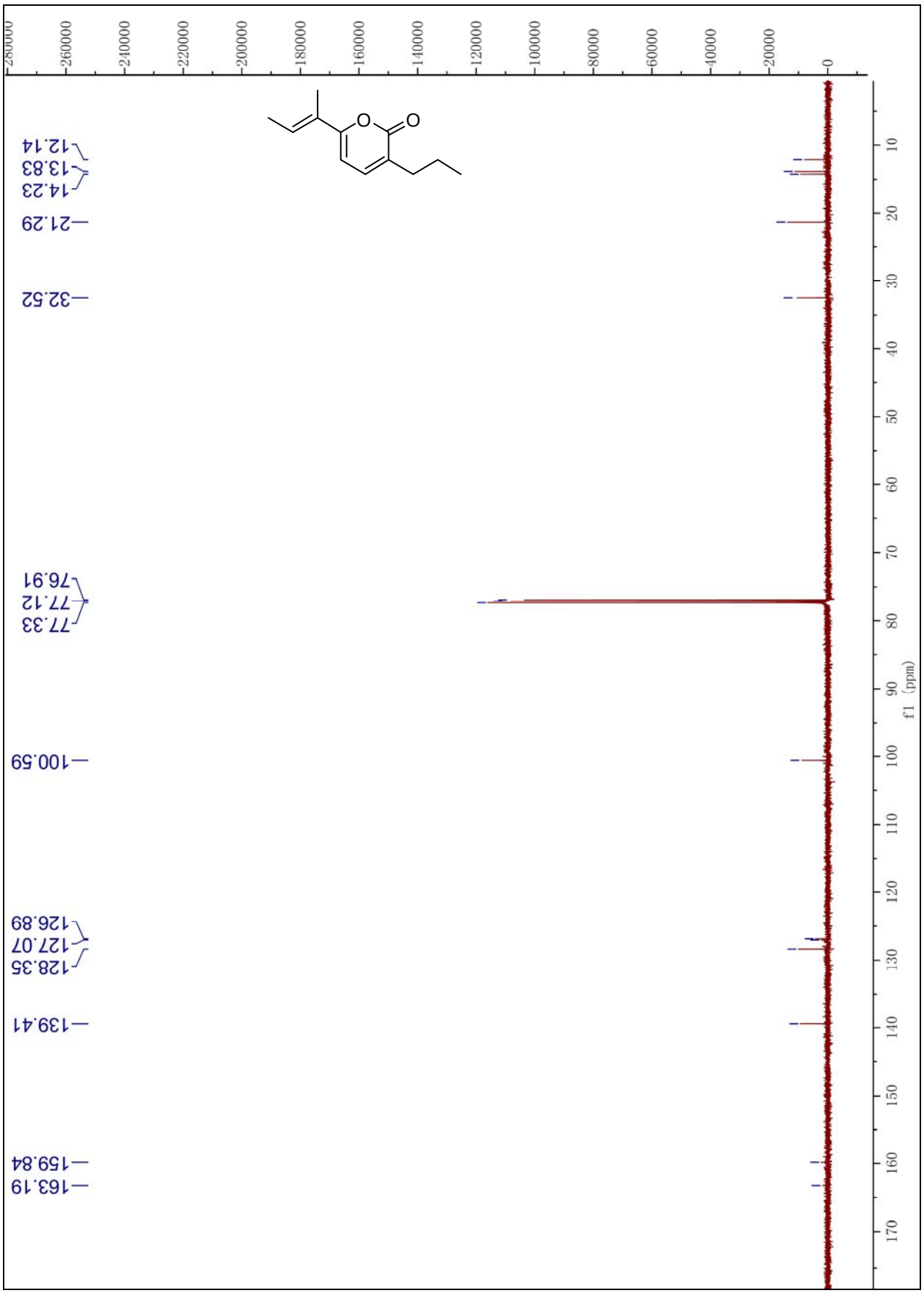

**Figure S16**. The DEPT spectrum of nocapyrone K (**4**) in $CDCl_3$ (150 MHz)

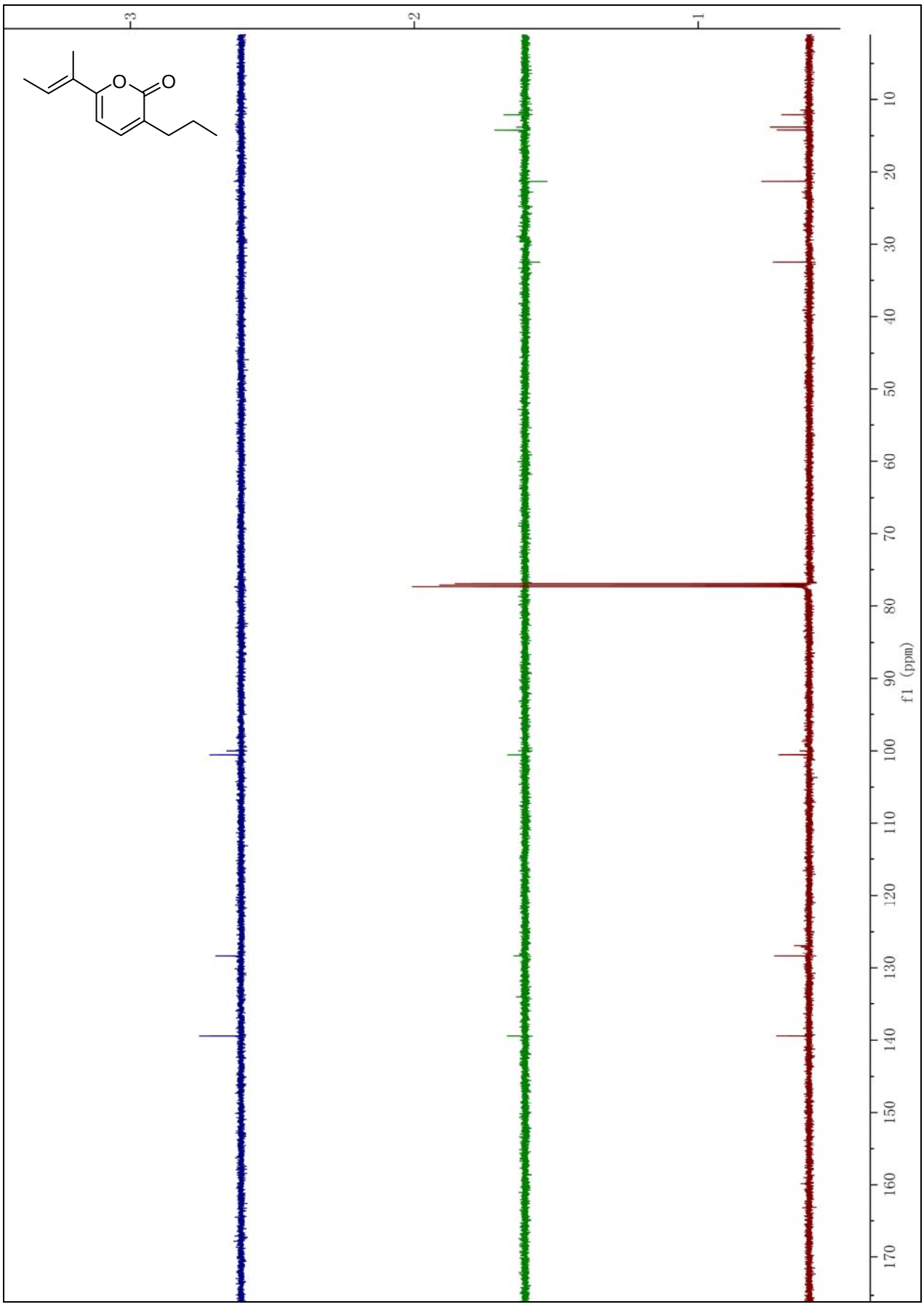

**Figure S17**. The $^{1}H$ NMR spectrum of nocapyrone L (**5**) in $CDCl_3$ (600 MHz)

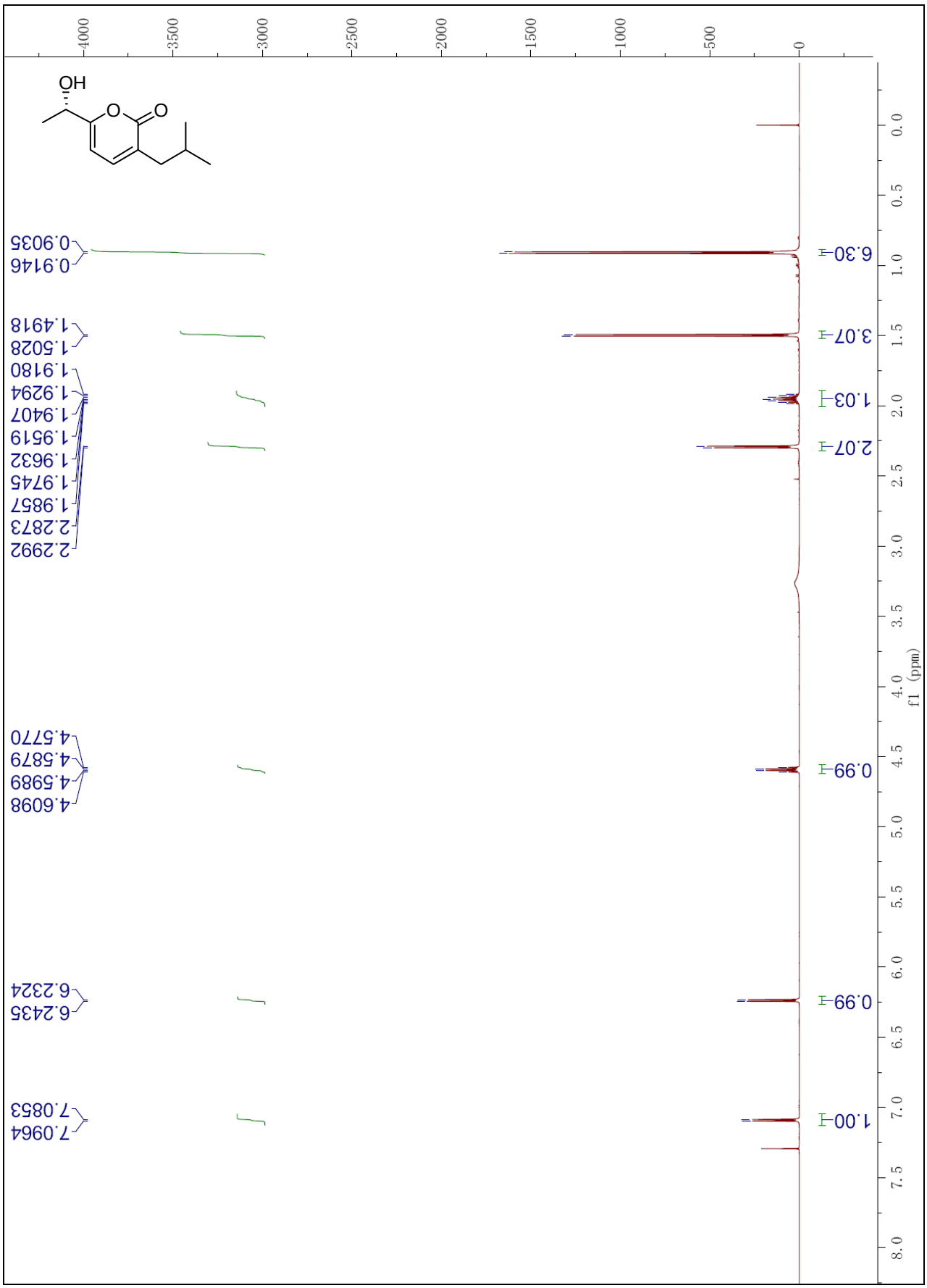

**Figure S18**. The $^{13}C$ NMR spectrum of nocapyrone L (**5**) in $CDCl_3$ (150 MHz)

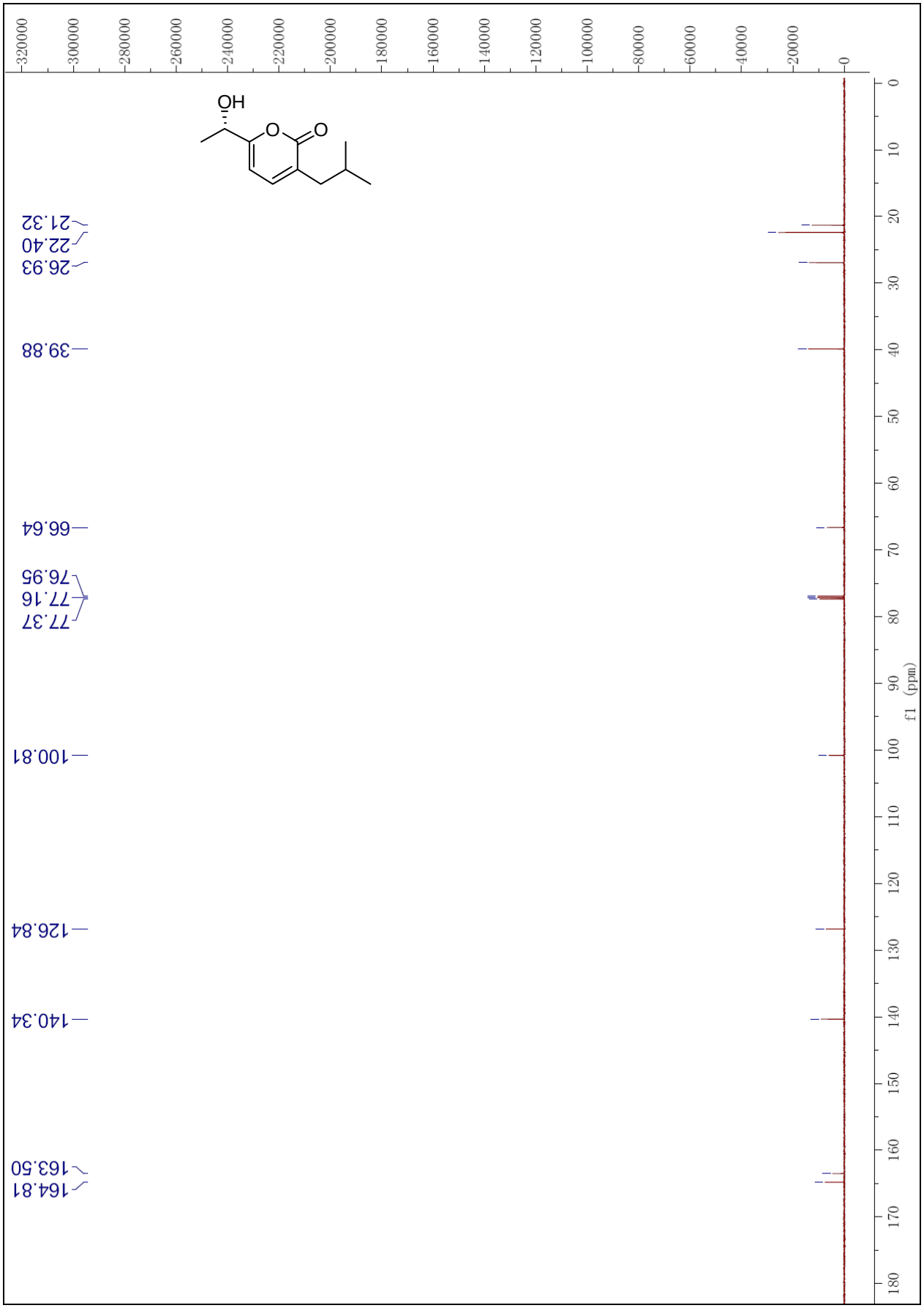

**Figure S19**. The DEPT spectrum of nocapyrone L (**5**) in $CDCl_3$ (150 MHz)

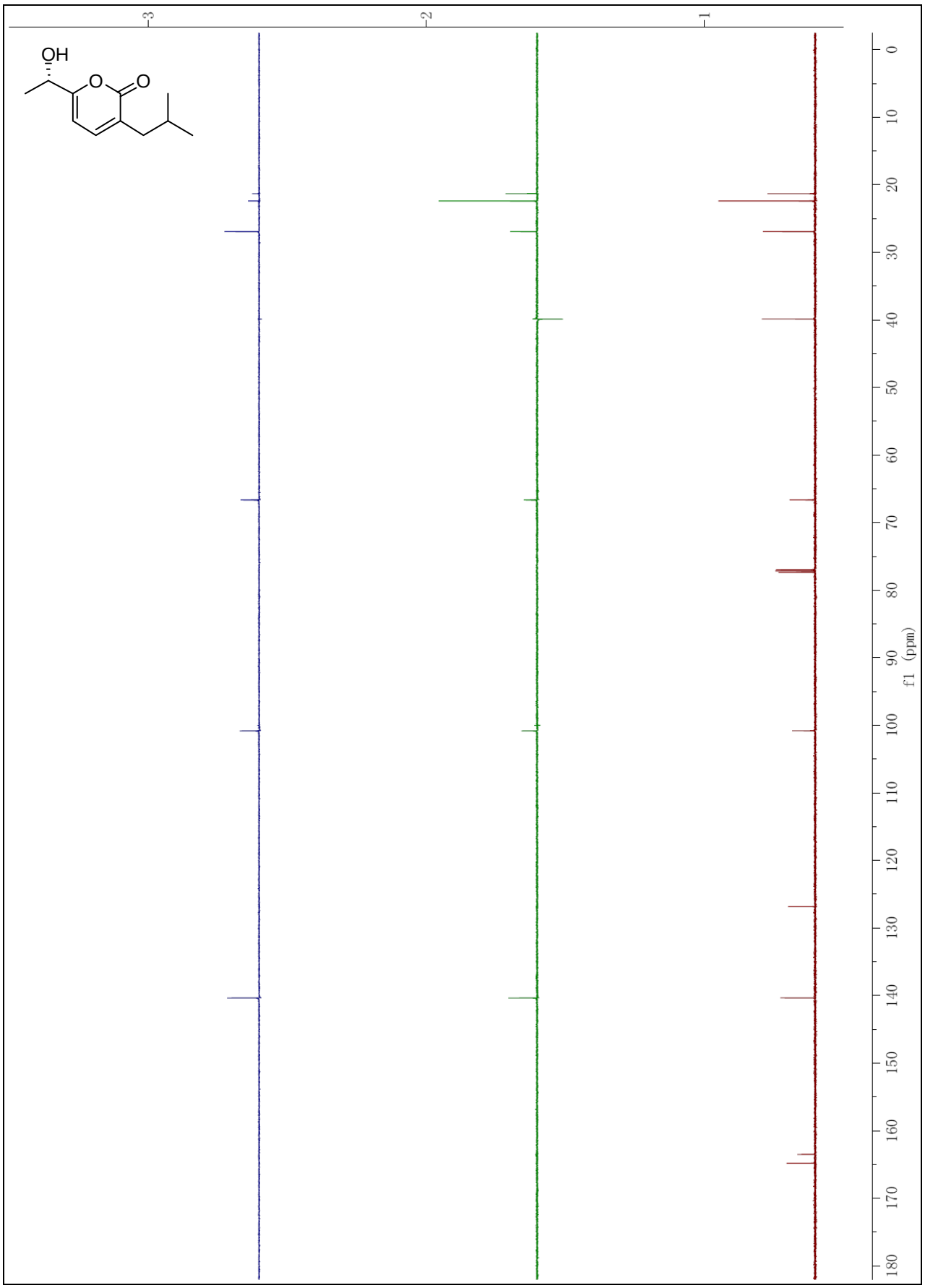

**Figure S20**. The $^{1}$H NMR spectrum of nocapyrone M (**6**) in $CDCl_3$ (600 MHz)

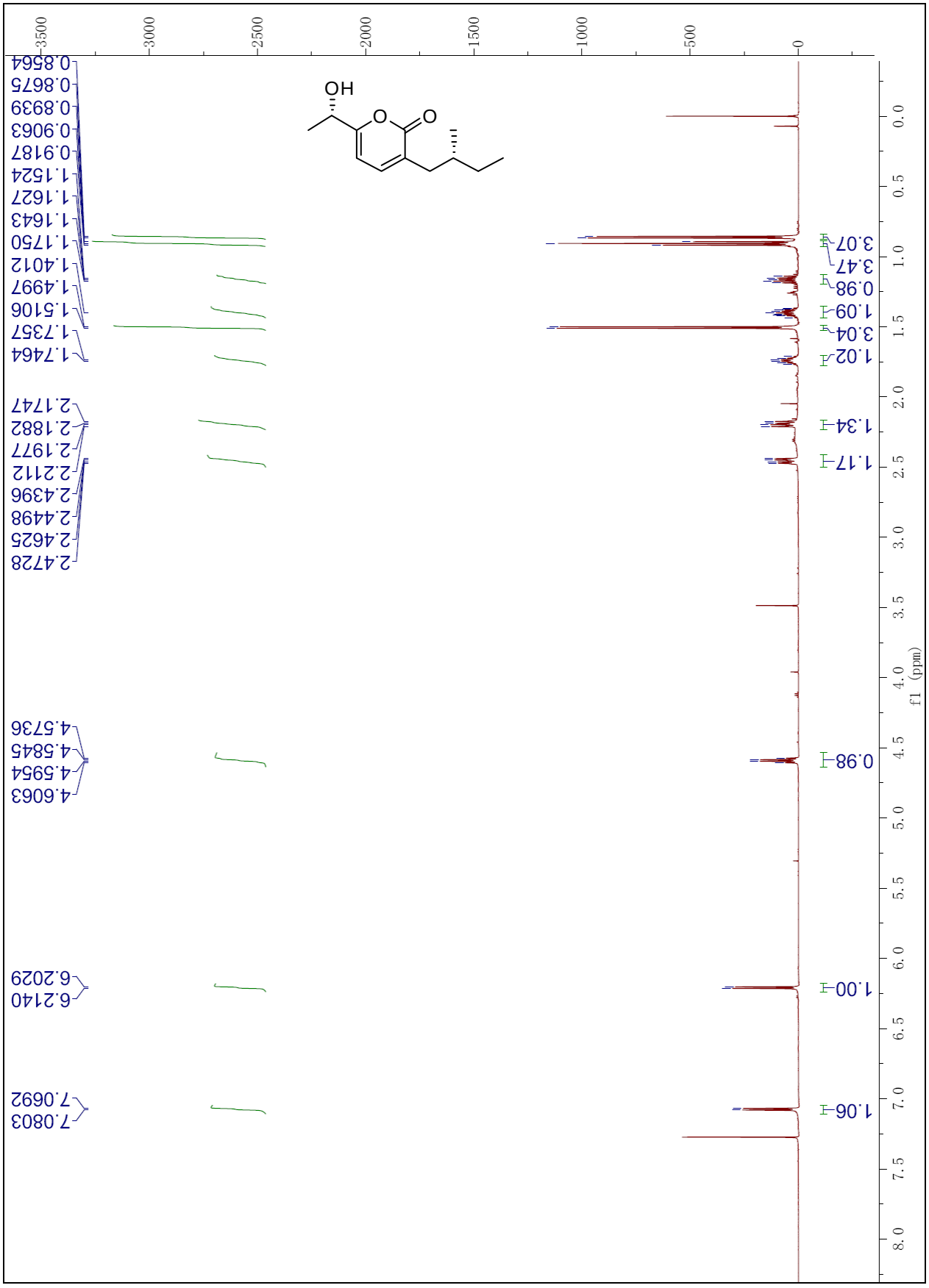

**Figure S21**. The $^{13}C$ NMR spectrum of nocapyrone M (**6**) in $CDCl_3$ (150 MHz)

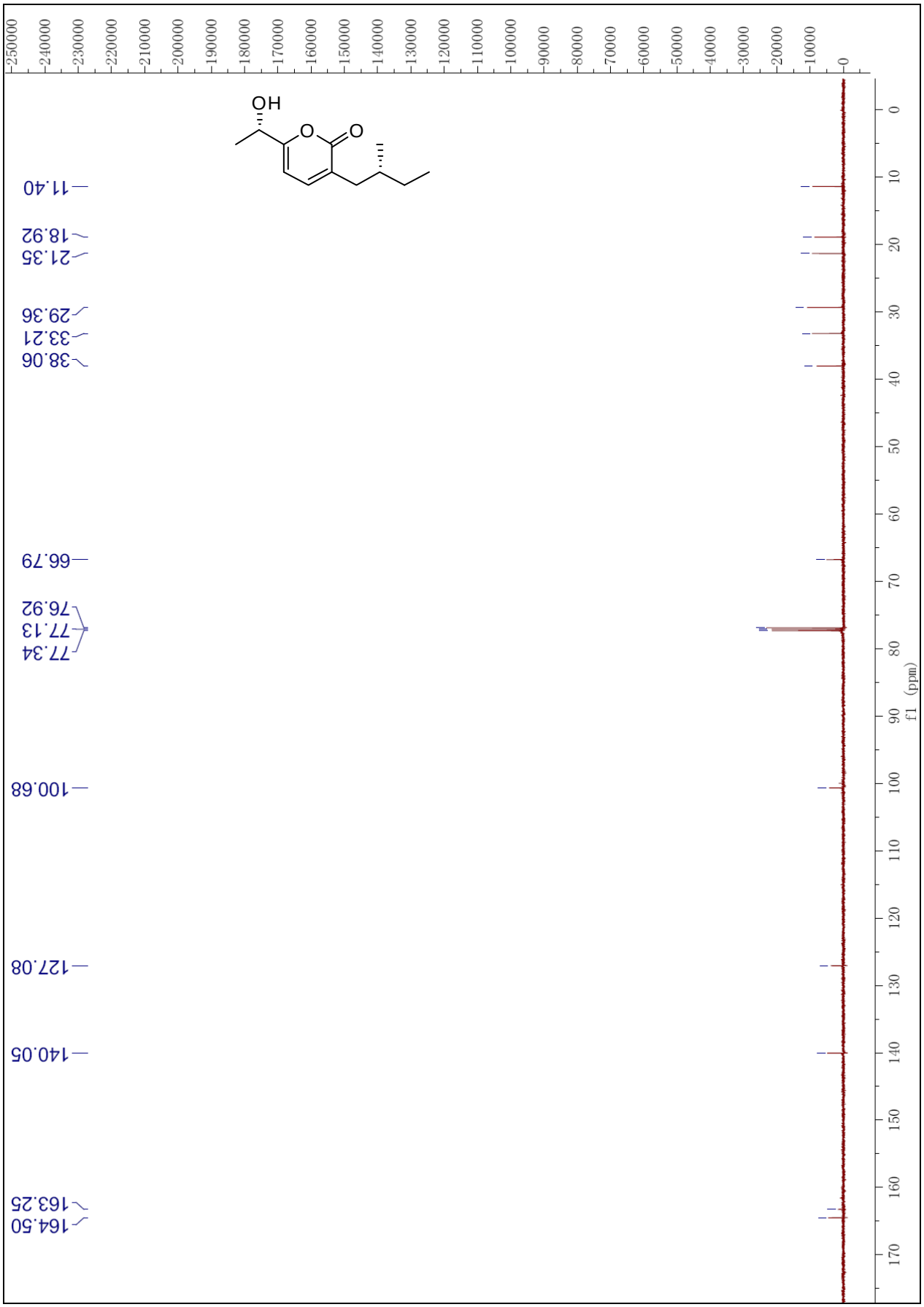

**Figure S22**. The DEPT spectrum of nocapyrone M (**6**) in $CDCl_3$ (150 MHz)

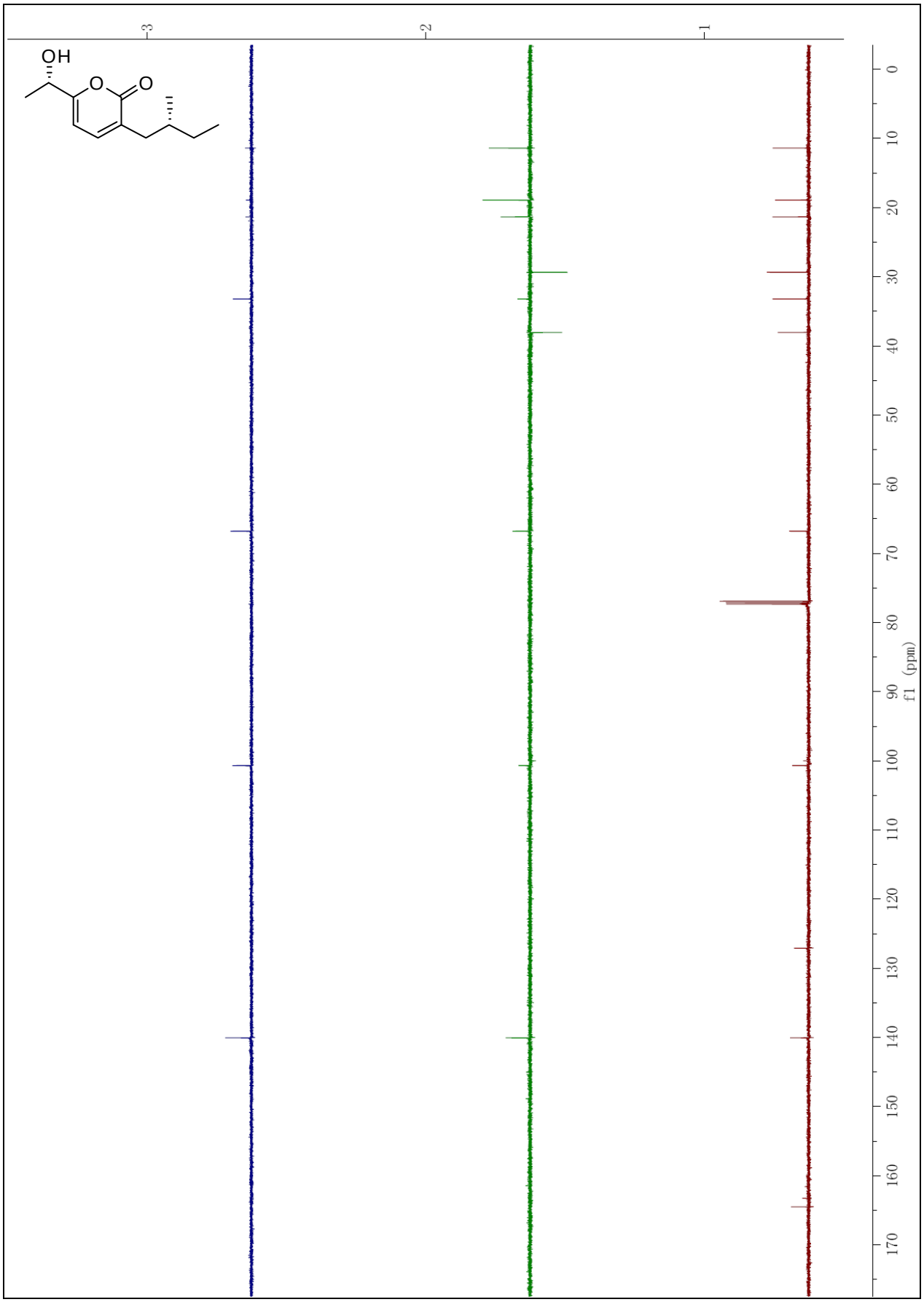

**Figure S23**. The $^{1}H$ NMR spectrum of nocapyrone N (**7**) in $CDCl_3$ (600 MHz)

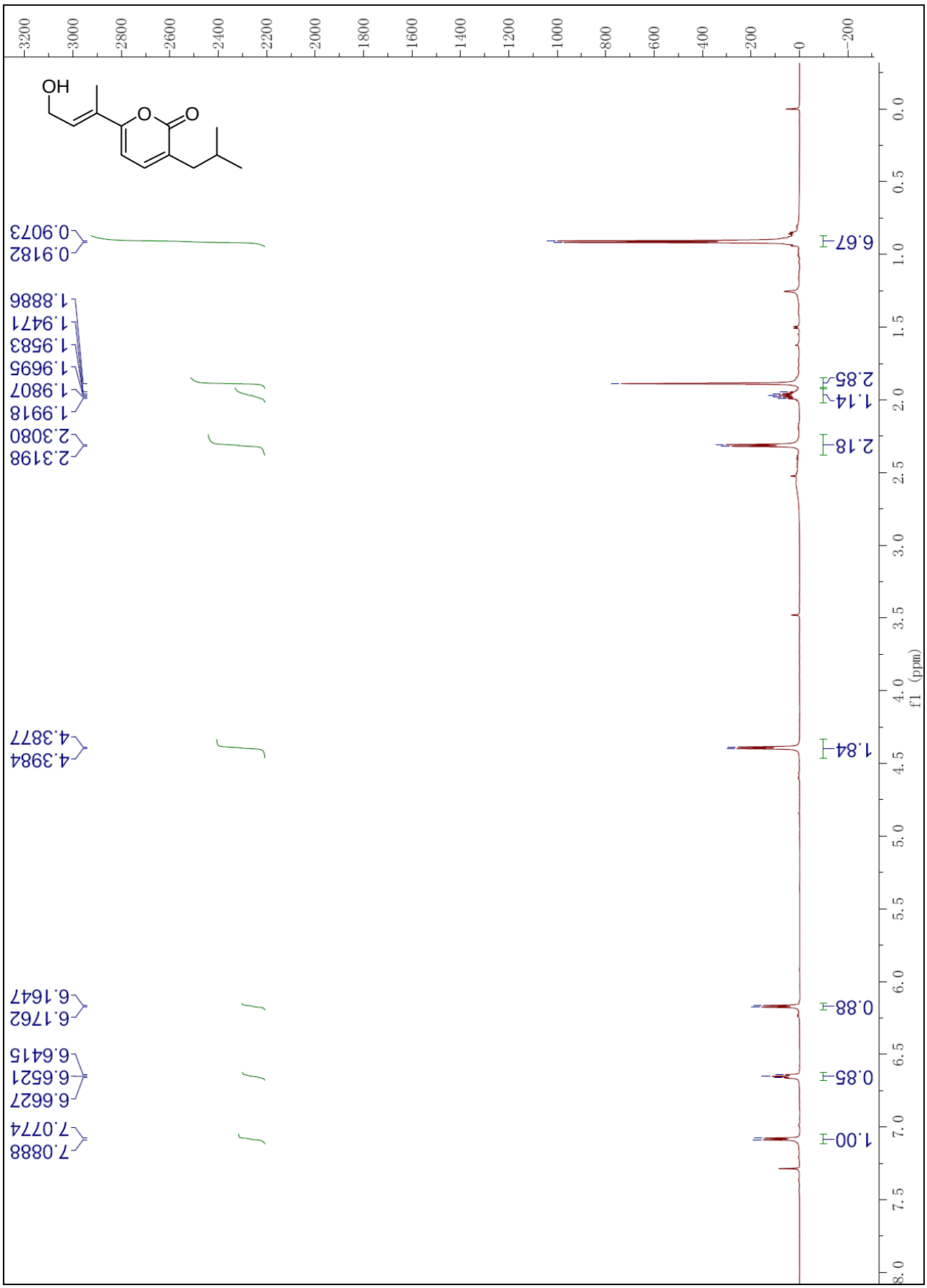

**Figure S24**. The $^{13}C$ NMR spectrum of nocapyrone N (**7**) in $CDCl_3$ (150 MHz)

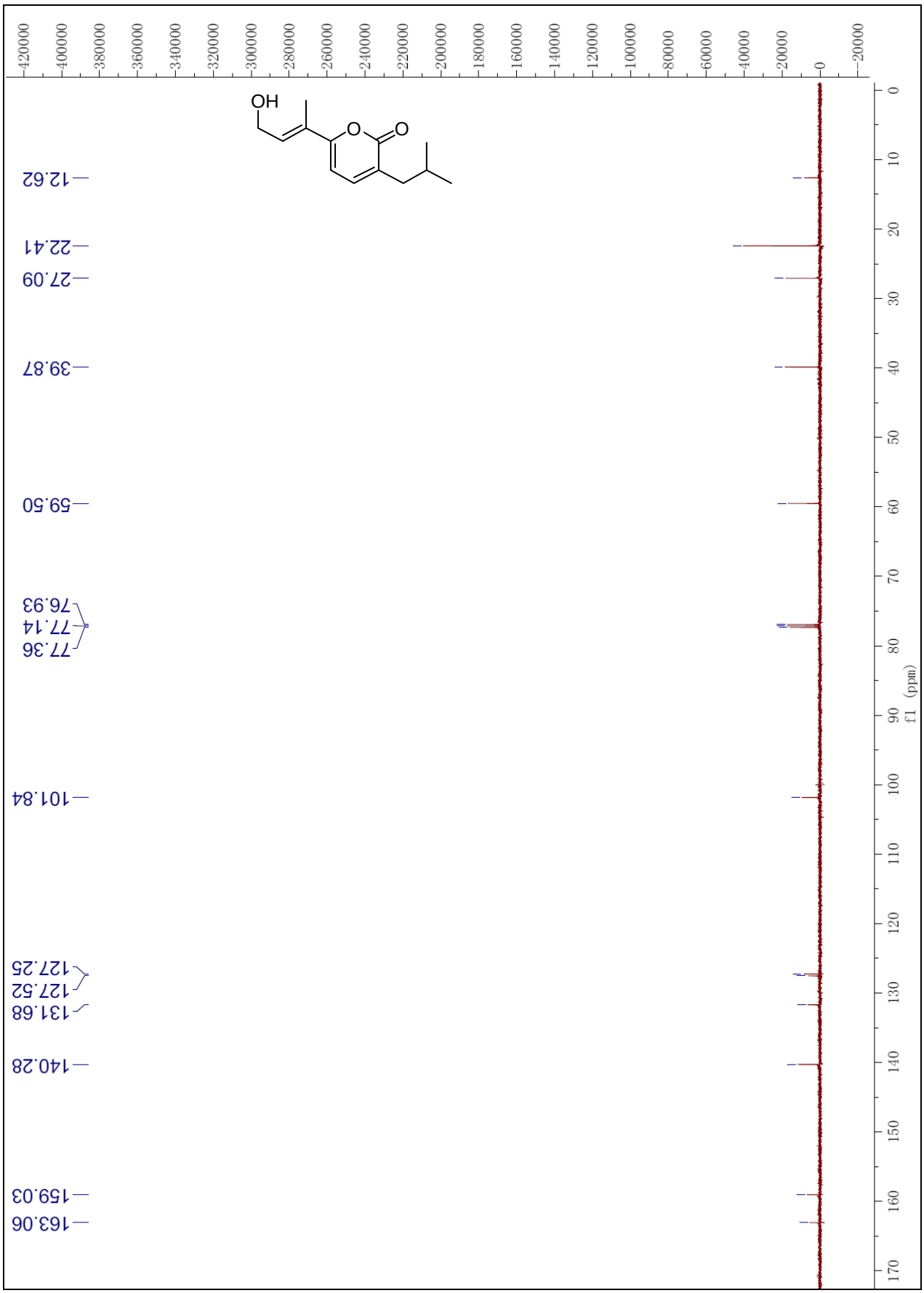

**Figure S25**. The DEPT spectrum of nocapyrone N (**7**) in $CDCl_3$ (150 MHz)

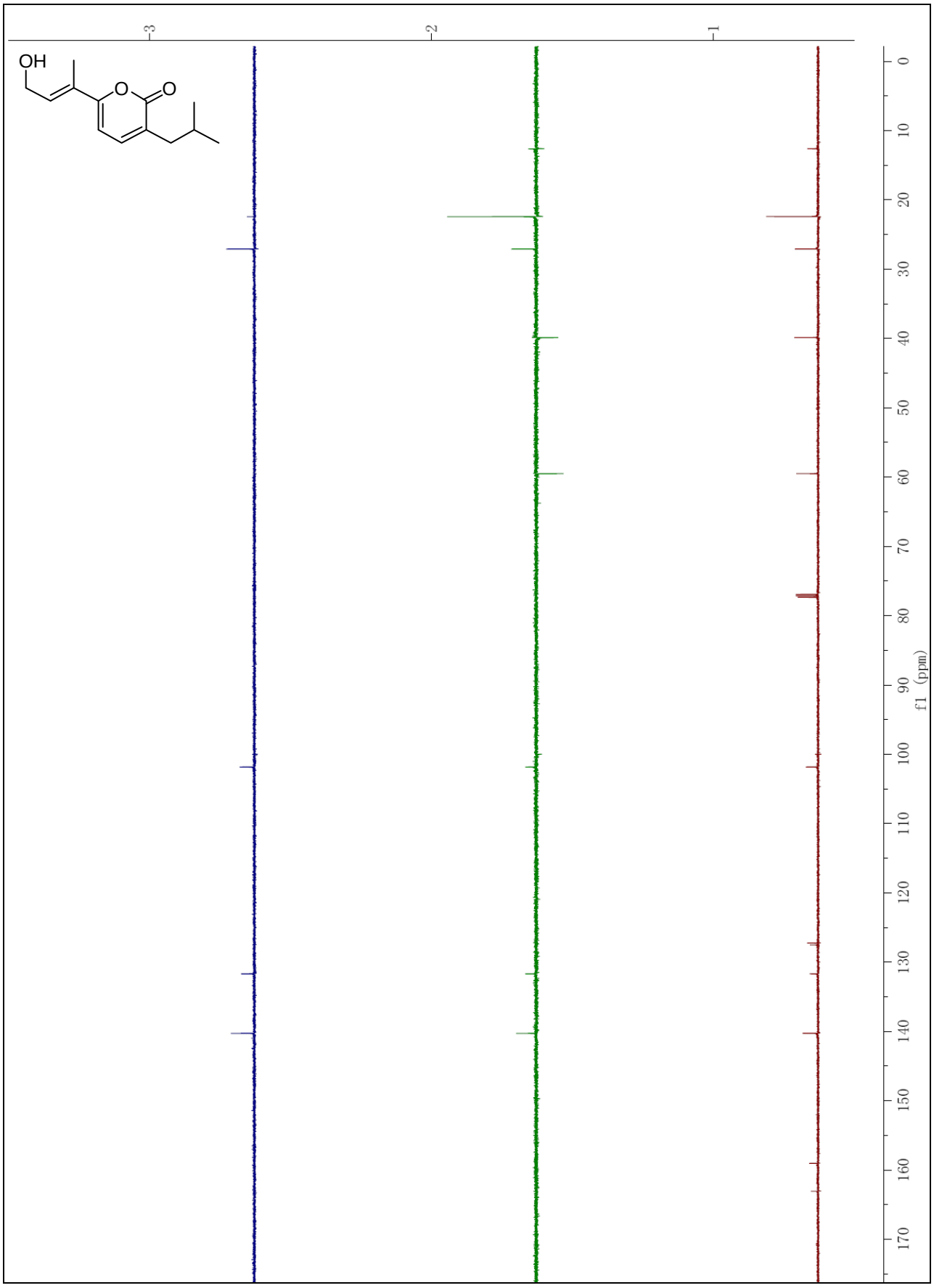

**Figure S26**. The NOE difference spectrum of nocapyrone N (**7**) in $CDCl_3$ (500 MHz)